

Scale Resonance: Effects of spatial scales on the inference of drivers behind species distribution

by

Fatumah Atuhaire

*Thesis presented in partial fulfilment of the requirements
for the degree of Master of Science in Applied Mathematics
in the Faculty of Science at Stellenbosch University*



Department of Mathematical Sciences,
Mathematics Division,
University of Stellenbosch,
Private Bag X1, Matieland 7602, South Africa.

Supervisor: Prof. Cang Hui
Co-Supevisor: Dr. Andriamihaja Ramanantoanina

December 2017

Declaration

By submitting this thesis electronically, I declare that the entirety of the work contained therein is my own, original work, that I am the sole author thereof (save to the extent explicitly otherwise stated), that reproduction and publication thereof by Stellenbosch University will not infringe any third party rights and that I have not previously in its entirety or in part submitted it for obtaining any qualification.

Signature:
Fatumah Atuhaire

Date: December 2017

Copyright © 2017 Stellenbosch University
All rights reserved.

Abstract

Scale Resonance: Effects of spatial scales on the inference of drivers behind species distribution

Fatumah Atuhaire

*Department of Mathematical Sciences,
Mathematics Division,
University of Stellenbosch,
Private Bag X1, Matieland 7602, South Africa.*

Supervisor: Prof. Cang Hui

Co-Supervisor: Dr. Andriamihaja Ramanantoanina

Thesis: MSc

December 2017

The factors that determine species distributions across landscapes have for long served keen interest to conservation biology. Abiotic factors have been the major determinants of species distribution at larger scales whereas biotic factors have been considered to be at small scales. The effect of a factor at one scale cannot be extrapolated to other scales. So to understand these effects, we need to make comparisons at multiple scales. Although there has been several progressive research studies done on the effects of spatial scales on species distributions, empirical studies involving varying more than one factor have been lacking. I develop a model that uses two factors of growth rate and carrying capacity as the key drivers of species distribution in a landscape. Each factor here has its own spatial autocorrelation and species' responses to these factors vary as the spatial scales increase from local to regional to global scales. I represent these factors as two fractal landscapes and implement an integro difference equation (IDE) on them. The results obtained tell us how the population density is dependant on the growth rate and carrying capacity.

Keywords: Spatial scale; fractal landscape; spatial autocorrelation; integro difference equations; hierarchical partitioning.

Uittreksel

Skaal Resonansie: Effek van ruimtelike skale op die afleiding van die bestuurders agter spesie verspreiding

Fatumah Atuhaire

*Departement Wiskundige Wetenskappe,
Universiteit van Stellenbosch,
Privaatsak X1, Matieland 7602, Suid Afrika.*

Tesis: MSc

Desember 2017

Die faktore wat die verspreiding van spesies oor landskappe bepaal, was vir lank 'n belangstelling van bewaringsbiologie. Abiotiese faktore beïnvloed hierdie verspreiding op die groot skaal, terwyl biotiese faktore vir die kleiner skaal in ag geneem moet word. Die effek van 'n faktor by een skaal kan nie geëkstrapoleer word na 'n ander skaal nie, so om hierdie effekte te verstaan, moet ons hulle op verskeie skale vergelyk. Alhoewel daar 'n hele paar progressiewe navorsingstudies oor die uitwerking van ruimtelike skale op die verspreiding van spesies gedoen is, ontbreek 'n empiriese studie waar meer as een faktor op 'n slag verander word. Ek ontwikkel 'n model wat die twee faktore van groeikoers en drakrag gebruik as die sleutelbestuurders van die verspreiding van spesies in 'n landskap. Elke faktor het hier sy eie outo-korrelasie en spesies se antwoorde tot hierdie faktore wissel soos die ruimtelike skale van plaaslik na streek na globaal vergroot. Ek stel hierdie faktore as twee landskappe voor en implementeer 'n integro versil (Eng. IDE) model op hulle. Die resultsate wat verkry word, vertel ons hoe die bevolkingsdigtheid afhanklik is van die groeitempo en drakrag.

Ruimtelike skaal; fraktale landskap; ruimtelike outokorrelasie; integro verskilvergelykings; hiërargiese verdeling.

Acknowledgements

First I will like to appreciate my supervisor Prof. Cang Hui. Without his help and timeless advice I would not have written this thesis. I am also glad that Dr. Andriamihaja Ramanantoanina offered very helpful comments and guidance as she co supervised my work. I thank Mrs Vanessa Du Plessis for the administrative help offered to me.

I am greatly indebted to AIMS-South Africa and NRF for funding this masters. In addition to the travel bursary awarded to me to attend a research school in Mathematical models for biology at University of Mauritius and the bursary top up from the SARChi chair, Prof. Cang Hui. None of the help received from you went unnoticed! Thank you!

Dedications

I dedicate this project to the God, who began a good work in me, has sustained it and has led it to accomplishment.

Contents

Declaration	i
Abstract	ii
Uittreksel	iii
Acknowledgements	iv
Dedications	v
Contents	vi
List of Figures	viii
List of Tables	ix
1 Introduction	1
1.1 Background of the problem	1
1.2 Motivation of the study	2
1.3 Research objectives	3
1.4 Project outline	3
2 Literature Review	5
2.1 Introduction	5
2.2 Definitions	6
2.3 Effects of change of scales on processes	9
2.4 Spatial autocorrelation	10
2.5 Fractal landscapes	12
2.6 Methods used to generate fractal landscapes	14
2.7 Summary	15
3 Model for generating and analysing fractal landscapes	16
3.1 Diamond square method	16
3.2 Integro difference equation (IDE)	19
3.3 Spatial dynamics of the IDE on the landscape	23

<i>CONTENTS</i>	vii
3.4 Statistical analysis of data generated	26
3.5 Summary	28
4 Scale Resonance	29
4.1 Introduction	29
4.2 Sampling Effect	29
4.3 Scaling Effect	36
4.4 Summary	42
5 Conclusion	44
5.1 Recommendations for further research	45
Appendices	46
A Codes For Simulation of Data.	47
A.1 Pseudo code for the generation of a fractal landscape.	47
A.2 Implemented code for the generation of a fractal landscape.	47
B Codes For Data Analysis.	50
B.1 Code implemented in generation of data (IDE);	50
B.2 Code for calculating the sampling effect	52
B.3 Code for calculating the scaling effect	56
List of References	63

List of Figures

2.1	Grain and extent of scale.	8
2.2	Spatial autocorrelation types	10
2.3	Patterns of spatial distributions.	11
3.1	Six steps of the diamond square method	18
3.2	Fractal landscapes when $h = 0.01$, $h = 0.5$ and $h = 1$	19
3.3	The Ricker growth curve with parameters $R = 1$ and $K = 10$;	21
3.4	Gaussian dispersal kernel.	23
3.5	IDE on a fractal landscape for Time 1 to 250	24
3.6	Population Size versus Time.	24
3.7	IDE on a fractal landscape for Time 1 to 50	25
3.8	Population versus Time.	26
4.1	Contribution of R (CR) and K (CK) to N and total variance explained (R^2RK) at different sample size.	30
4.2	An example plot of the contributions of R and K as the function of the sample size.	30
4.3	Moran's I of R (MR), K (MK) and N (MN) at different sample sizes.	31
4.4	FDR, FDK and FDN at different sample sizes.	33
4.5	Regression coefficients of Moran's I (RC1) and FD (RC2) at different sample sizes.	35
4.6	Contributions of Moran's I (HP1) and FD (HP2) at different sample sizes	36
4.7	Contribution of R (CR) and K (CK) to N and total variance explained (TV) at different merged grids.	37
4.8	An example plot of the contributions of R and K as function of the merged grids. Blue and red correspond to R and K respectively.	37
4.9	MR, MK and MN as functions of merged grids.	38
4.10	FDR, FDK and FDN for different merged grids.	40
4.11	Regression coefficients of Moran's I (RC3) and FD (RC4) for different merged grids.	42
4.12	Contributions of Moran's I and FD for different merged grids.	42

List of Tables

2.1	Example of commonly used scales as proposed by Hortal <i>et al.</i> (2010).	8
3.1	Descriptions of parameters and variables.	22
4.1	Regression coefficients from <i>MR</i> , <i>MK</i> and <i>MN</i> at different sample sizes. Refer to RC1 in Figure 4.5.	32
4.2	p-values of <i>MR</i> , <i>MK</i> and <i>MN</i> at different sample sizes.	32
4.3	Joint and individual contributions at different sample sizes. Refer to HP1 in Figure 4.6.	33
4.4	Regression coefficients from the FDR and FDK at different sample sizes. Refer to RC2 in figure 4.5.	34
4.5	p-values of FDR and FDK for different sample sizes.	34
4.6	Joint and individual contributions of FDR and FDK at different sample sizes. Refer to HP2 in Figure 4.6.	35
4.7	Regression coefficients from MR and MK for different merged grids. Refer to RC3 in Figure 4.11	38
4.8	p-values of MR and MK for different merged grids.	39
4.9	Joint and individual contributions of <i>MR</i> , <i>MK</i> and <i>MN</i> for different merged grids. Refer to HP3 in Figure 4.12.	39
4.10	FDR, FDK and FDN for different merged grids. Refer to RC4 in Figure 4.11.	40
4.11	p-values of FDR and FDK at different merged grids.	41
4.12	Joint and individual contributions from FDR and FDK for merged grids. Refer to HP4 in Figure 4.12	41

Chapter 1

Introduction

1.1 Background of the problem

The beauty of nature before our eyes is often represented in terms of scale. Like Albert Einstein said, "Look deep into nature and you will understand everything better." Ecologists have come to realise that ecological phenomena and processes entirely depend on scale and this has driven keen interest on applications of scale (McGill *et al.*, 2010). This concept has been vital in influencing ecological studies, interpretation of results and bridges a gap between processes at different scales. According to Levin (1992), relating patterns across scales is the main problem in Ecology and in all other sciences. Generally, theoretical sciences entail relating processes that are seen on several distinct scales of time, space and organizational complexity.

Hutchinson (1965) related processes and patterns in terms of an ecological theatre such that the drama played depends on different scales, and the ability to comprehend the drama requires that it is viewed on the right scale (Wiens, 1989). It is crucial for us to understand how problems and solutions depend on scales so we can in turn manage and conserve biodiversity.

At one scale it may be changes in climate, while at another it may be habitat loss and fragmentation or disturbance that need to be addressed (Henle *et al.*, 2014). For example work done by Suarez *et al.* (2001), showed that the distribution of Argentine ants is affected by species turnover of native ants at local scale. Precipitation, temperature and topology influenced the regional scale whereas climate suitability and human footprint determined the global scale.

Although theoretical work has been done on the relevance of scales in understanding nature, the ecological applications of these scales has been rampant only recently maybe because ecologists have been confined to traditional methods (Wiens, 1989).

Species distributions and interactions are predicted basing on the patterns across spatial scales (Wisiz *et al.*, 2013). This is because they are not random

but rather correlated in space and time. The distributions of species into patterns are influenced by several biotic and abiotic factors. For example climate as one of the primary causes of species distributions, is abiotic factor that can be observed at fine scales (Wiszniewski *et al.*, 2013).

Species distribution models (SDM) have been used to model how species respond to changes in the environment as well as understanding the effects related to changes in grid size. Studies done by Guisan *et al.* (2007) showed that changes in the scale size have minimum effect on the SDM performance and review of grid size effects on the factors that determine species distribution have not been examined yet.

In this project we explore an individual species that has non-random, aggregated patterns in which the environment is heterogeneous. The change in species distribution characteristics as the grain of sampling change, are our major concern here. When there is an increase in scale, the question of matter is how does this increase affect the deductions we make on factors that drive species distribution?

1.2 Motivation of the study

Maintenance of ecological systems requires a deep understanding of how species distribute and interact. This is so for the purposes of conservation and climate change management. Thus this has influenced modellers to conduct continuous and progressive evaluation of the statistical models predicting species distributions (Austin, 2007).

Several researchers believe that species distribution models based on statistical analysis, without including ecological contributions and effects are insufficient for making meaningful prediction (Sinclair *et al.*, 2010). This has driven the evaluation of models to be based on ecological theory, type of data and statistical methods.

Studying species distributions is of key interest especially in conservation planning for example with existence of rare or endangered species (Chevalier *et al.*, 2014).

There are several mechanisms that explain species distributions including species interactions, environmental gradients, historical factors, land cover, dispersal among others (Kamino *et al.*, 2012). One of the challenges in modelling species distribution is the selection of the relevant predictors (Kamino *et al.*, 2012). This is because not all factors influencing species distributions can be extensively formulated as predictors.

This study seeks to address this challenge by choosing two key factors of carrying capacity and growth rate and analysing them at different spatial scales. These predictors are affected with the existence of collinearity and this can lead to misidentification of the most relevant predictors. We tackle that by using a generalised linear model to investigate the relationship between the

two variables and population and this in the end tells us the contribution of each variable to population.

Empirical studies have shown that these factors are affected by spatial scales and the location at which the study is done. For example taking two climatic variables say rainfall and temperature; temperature too appears to be less strongly synchronized between sites relatively close together than rainfall, but is slightly more synchronous between sites farther apart (Koenig, 2002). More so temperature exhibits high synchrony declining with distance and are statistically significant over large distance, often on a global scale.

We are able to explain the patterns existing in nature using fractal landscapes by understanding how these variables vary at different scales to determine species distributions. Inclusion of spatial autocorrelation validates the basis on which neighbouring species look more similar than those far from each other.

1.3 Research objectives

The aim of this research is to investigate how the change of spatial scales affects factors influencing species distribution. In this project, the main objectives are:

- To describe the combined and relative influence of variables to influencing species distribution across scales,
- To predict how regression coefficients change as a function of grain and extent,
- To evaluate how population, depends on variables of carrying capacity and growth rate,
- To introduce what the concept of scale resonance is,
- To assess how change of scale influences the factors that lead to species distribution.

1.4 Project outline

In this project, we start by introducing spatial scales, what they are and their implication in understanding species distribution. We explore and review scales, processes and patterns. We also review the common examples of effects of scale on ecosystems. Thereafter, we review species distributions and the history behind the methodology of use in this study.

Chapter three describes the model used and there we introduce fractal landscapes; that is as a representation of natural terrain. Briefly we explain the different methods used in generation of fractals scaling down to diamond

square algorithm for our usage. We use these fractals to represent growth rate and carrying capacity as the main factors that affect population dynamics. We shall explore spatial temporal models but in particular our focus being on the integro difference model for modelling growth and dispersal in species distributions. We show numerical simulations of the spatial temporal dynamics of the integro difference model on fractal landscapes. Finally the methods used to generate data which we shall use in chapter 4.

In chapter four, we analyse the contribution of each variable to the population density. Then we calculate the spatial autocorrelation at different scales using Moran's I. The effect of changing spatial scales, sampling effect and fractal dimension is investigated. There after we investigate the relationship between the two variables and the population density using statistical methods of the generalised linear model.

In chapter five, we conclude by presenting our major results from the research and summarising inferences drawn from these results.

Chapter 2

Literature Review

2.1 Introduction

In the ecologist's quest to study the mechanisms that generate observable repeatable patterns and what causes them, there was need to assign processes to a hierarchy of scales. This could only be effective if these processes were studied on the right scale. However, increasing evidence of processes operating and interacting across scales has revealed that there is no right scale ([Hewitt *et al.*, 2010](#)).

According to [Levin \(1992\)](#), since an appropriate scale is not automatic, systems generally show characteristic variability on a range of spatial, temporal and organisational scales. Some of the variables considered when determining which scale to use include the available data and the system used ([Elith and Leathwick, 2009](#)). Although this does not mean that all scales are equal or that there is no scaling laws that governs them. It actually explains why the concept of scale has been widely used as a major matter of interest in understanding landscape ecology since its recognition in the late 1970's and 1980's ([Schneider, 2001](#)).

Scale is one of the most widely used words in ecology. It is a universal concept that cuts across most natural and social sciences ([Wu *et al.*, 2006](#)). According to [Schneider \(2001\)](#), the recognition of scale occurred rapidly in the 1980's, although the concept in itself is much older. This fast growing recognition has led to publishing of several books, journal papers and articles which have contributed significantly to our current understanding of matters pertaining to scale.

There is a seemingly growing consensus in ecology that pattern and process make little sense without consideration of scale ([Wu *et al.*, 2006](#)). While scale issues are widely recognized, a comprehensive description of scale effects and applications still is missing.

The aim of this chapter is to offer a detailed explanation of what spatial scales are, explain the effects of their change on processes and patterns. There

after, we introduce spatial autocorrelation and Morans I coefficient. We will then introduce the concept of fractal landscapes, history and then review the methodology of generating them.

2.2 Definitions

Several scholars have explained scale in terms of its nature, uses and applications in ecology. Some definitions of scale include;

- The spatial extent of an ecological process indexed by space and time (Wiens, 1989),
- The grain of a variable explained by time or space (Schneider, 2001),
- The distance before some quantity of interest changes (Powell, 2001).

Scale in terms of its characteristic, dimension and components is explained below.

2.2.1 Characteristic scale

The characteristic scale is the scale at which dominant patterns emerge or the scale at which maximum spatial variance among locations elapses (McGarigal, 2016).

According to Jager (2007), ecological patterns and processes should be addressed at their characteristic scales since the dynamics of these processes are independent of each other. The characteristic scale can be detected using method of fractal analysis (Wu and Li, 2006).

Most ecological studies explain scale in terms of dimension of space and time without considering the organisational level. The ratio between these two scales tends to remain unchanged over a range of scales since the characteristic scale of most ecological processes are related in space and time (Jager, 2007). The organisational levels have to be uniform with spatial and temporal scales for scaling to be effectively done.

2.2.2 Types of scale

Scale can be explained in different types much as they are all related to each other in several ways. The intrinsic scale is the scale on which patterns or processes operate (Wu and Li, 2006). However, some scholars argue that there is no intrinsic scale in nature, but rather scales are only consequences of the observer. According to Wu and Li (2006), the observed scale of a given occurrence is due to the interaction between the observer and the natural scale.

The measurement scale is the scale at which measurement is taken while the experimental scale is represented BY the spatial and temporal dimensions

of an experimental system (Wu and Li, 2006). When the scale of observation and analysis are properly chosen, the characteristic scale of phenomena of interest will be detected correctly (Jager, 2007).

2.2.3 Components of Scale

Scale can also be explained in terms of the extent of analysis, as the resolution in space or time of statistical analyses and models. For a better understanding of dimensions of scale and types of scale, we employ components of scale.

Scale in terms of its components takes several of them although, grain and extent are the most crucial since ecology and most of the earth sciences studies describe it like that.

Grain is defined as the size of specific units of observation (Wiens, 1989). It is the finest component of the environment that can be differentiated up close by an organism. In terms of area, it is the smallest area over which the average value of a variable is derived. It describes the properties of data like the spatial accuracy of species records, the predictor variables and their grid cells, (Elith and Leathwick, 2009); (McGarigal, 2016).

Extent reflects the importance of the analysis. It is the spatial domain or the geographical scale over which the system is studied (McGarigal, 2016). In other words, it is the range at which a relevant object can be distinguished from a fixed view point by the organism.

Grain and extent determine the limits of resolution of data that is fine and coarse scales respectively. The two aspects are correlated and are key to the study of heterogeneous landscapes (Jager, 2007). Figure 2.1 is an illustration of scale in terms of extent and grain.

To scale from habitat to landscape and beyond, we seek to know how information is transferred from small scales to large scales and vice versa. It is therefore important that we learn how to aggregate and simplify key information without getting entangled with unnecessary details (Levin, 1992).

2.2.4 Example of commonly used scales.

Many environmental processes depend on scale which makes it essential while characterizing geospatial data (Koenig, 2002). The Table 2.1 is an example of categories of scale although this is always changing depending on the area and the research being conducted.

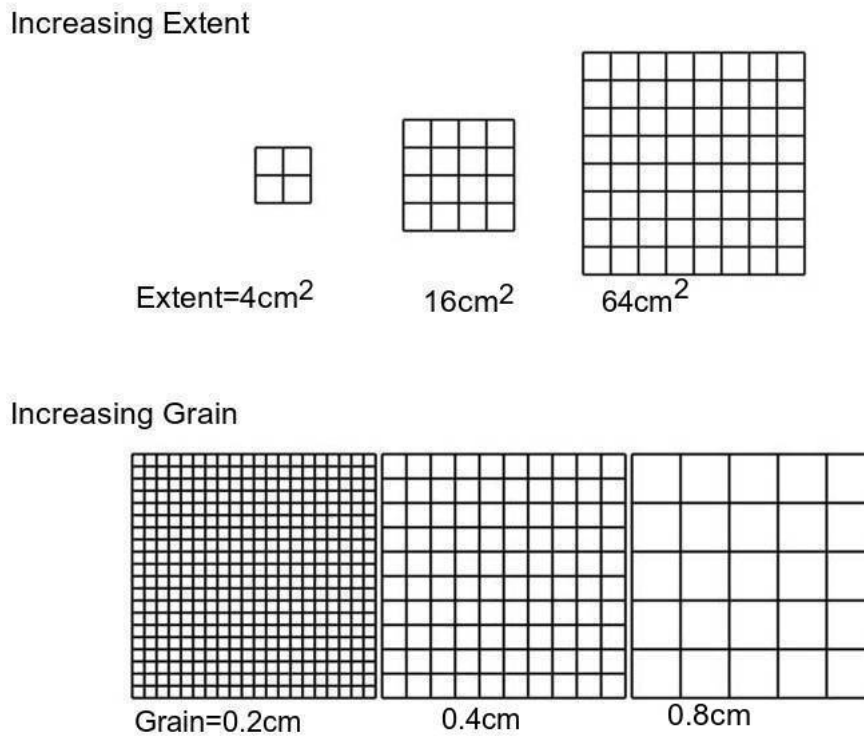


Figure 2.1: Grain and extent of scale.

Table 2.1: Example of commonly used scales as proposed by [Hortal *et al.* \(2010\)](#).

Example of commonly used scales	
Scale	Area
Point	$< 10^1\text{m}$
Site	$10^3 - 10^1\text{m}$
Local	$10^4 - 10^3 \text{m}$
Landscape	$2 \times 10^5 - 10^4\text{m}$
Regional	$2 \times 10^6 - 2 \times 10^5\text{m}$
Continental	$10^7 - 2 \times 10^6\text{m}$
Global	$> 10^7\text{m}$

2.3 Effects of change of scales on processes

Spatial and temporal dimensions of ecological phenomena are key in the conceptual framework of ecology although, it is only recently that they have been explicitly incorporated in building ecological theory and design (Chave, 2013). After identifying the relevant scale at which patterns and processes from natural systems result, models that bridge across scales are then developed. Change in scale leads to emergence of new processes in addition to changes in the existing ones.

The controls on patterns and processes may change with changes in scales. This can be influenced by the existence of biological interactions which separate systems from directly determining patterns (McGarigal, 2016). For example the relationship among climatic variables that are observable at larger scales may disappear at smaller scales, overridden by ecological processes, spatial or temporal lags. Thus observations made at small scales end up missing important patterns and processes operating at larger scales. More so, large scale observations may not have enough details necessary to understand small scale dynamics and vice-versa (McGarigal, 2016).

The change of scale may also cause statistical relationships to change. For example, new patterns emerge at several scales of investigation of an ecological system. When the scale of measurement of a variable is changed, we see changes in aspects like the signs of correlations, spatial variance and variance relationships of variables (McGarigal, 2016). As illustration, according to Levin (1992) the spatial distributions of krill populations of the Southern Ocean were shown to be patchy on almost every scale of description and their variability showed that variance decreases with scale. This suggests that an increase in grain of measurement lead to decrease in spatial variance while holding extent constant.

We could go on and on with more examples but the persistent issue to notice here is that different patterns exist at different scales of study in most aspects of ecological systems. This effect is a key determinant in the distribution of species. Understanding the transition of dynamics across scales in ecosystems is still a challenge and several papers in the past have tried to address this issue (Chave, 2013).

There has been progressive work done by ecologists for the last 40 years that indicates that biotic interactions predominantly play a key role in shaping patterns at local scales whereas abiotic factors like climate change operate more at regional or broader scales (Wisz *et al.*, 2013). However, not much attention has been paid to analysing the variations when two key factors are occurring together (Amissah *et al.*, 2014).

2.4 Spatial autocorrelation

Spatial autocorrelation (SA) is the measurement of how similar objects close to each other are. As the distance between two neighbouring variables M and N decreases, their values tend to be similar and vice versa.

SA is often times explained as distance decay of similarity. Objects far apart tend to be independent while as those near each other tend to be dependent. Waldo R. Tobler's first law of geography which states that "everything is related to everything else, but nearby objects are more related than distant objects" summarizes the concept of SA.

Moran (1950) categorised SA into three following groups;

- Positive SA, which occurs when the value at one location is similar as that in a neighbourhood location. There is dependence of the data variables on each other and so the distribution pattern will be clumped as illustrated in Figure 2.2a. One example of positive SA is seen in data clusters.
- Negative SA, occurring when the value at one location is different from that of a nearby location. There is independence in the data variables and this indicates a dispersed pattern of distribution as illustrated in Figure 2.2c.
- No SA, in which case the spatial autocorrelation is non existent leading to a random distribution pattern as illustrated in Figure 2.2b.

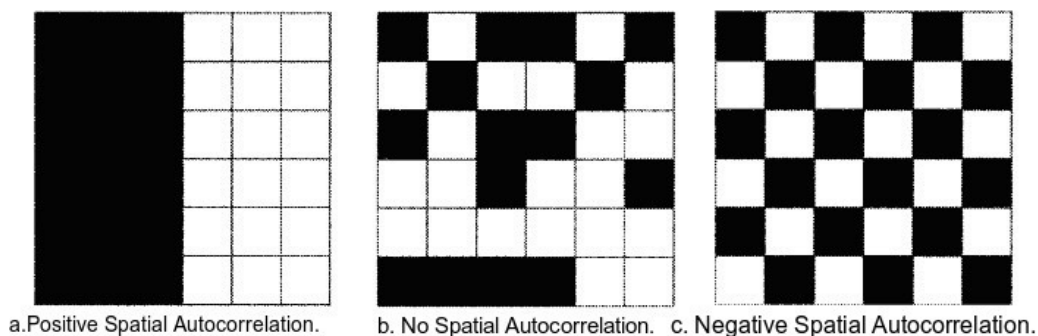


Figure 2.2: Spatial autocorrelation types

F Dormann *et al.* (2007) explained some of the causes of spatial autocorrelation in data as;

Environmental factors, like dispersal and extinction are distance related which make elements interact within a near by geographical dimension hence resembling each other.

When the choice of the data is non random. That is data is selected as opposed to randomly picked. This may lead to several data picked from a location clustered together.

SA as viewed in terms of species arranged is shown in Figure 2.3 where clumped distribution portrays a positive SA, uniform distribution portrays a negative SA and random distribution explains no SA.

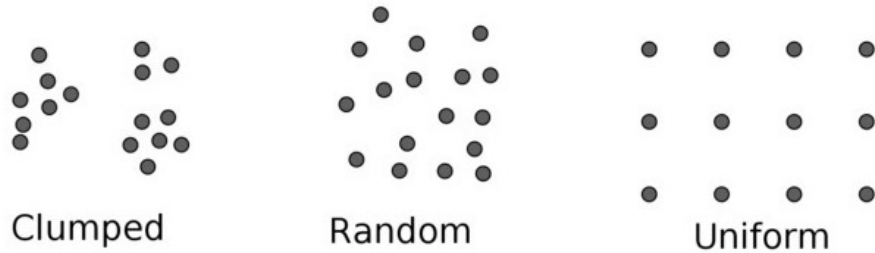


Figure 2.3: Patterns of spatial distributions.

2.4.1 Moran's I coefficient

SA can be assessed using indices like the joint statistics, Geary's C, general cross product statistic and correlation gram, but for this project we shall use Moran's I (Sawada, 2004).

Moran's I is used to measure of global SA. It depends on the feature locations and attribute values. Mathematically it is given by (Moran, 1950)

$$I = n \frac{\sum_{i=1}^n \sum_{j=1}^n w_{i,j} (z_i - \bar{z})(z_j - \bar{z})}{\sum_{i=1}^n \sum_{j=1}^n w_{i,j} \sum_{i=1}^n (z_i - \bar{z})^2} \quad (2.4.1)$$

Where

n is the total number of observations.

$w_{i,j}$ is the weight between observations i and j . Here we use the inverse of the distance between two cells.

i and j are locations.

z_i is the observation at location i .

z_j is the observation at location j .

\bar{z} is the mean of all observations, z .

The Morans coefficient I , will take on values ranging from -1 to 1 . If the observed value is 0 , 1 and -1 , that is an indication of no SA, positive SA and negative SA, respectively.

2.4.2 Implications of spatial autocorrelation

Statistics is based on the assumption that variables are independent of each other. Existence of SA violates this assumption. SA is important in understanding the nature and strength of these interdependencies so as to make valid inferences.

SA has been applied in analysing the spread of disease or an trend in ecology. For example, to attest whether the disease or trend is spreading, or is concentrated.

2.5 Fractal landscapes

In most physical systems, the arrangement of patterns changes in detail at different scales, but keeps statistically "self-similar" if the differences in pattern measurements are adjusted to the differences in the scale of measurement (Wiens, 1989). In addition, classical euclidean geometry does not effectively describe spatial patterns. This is because these patterns are fragmented and highly irregular in nature (Scott *et al.*, 2006). The development of fractals was a way of describing such complex natural patterns.

Benoit Mandelbrot's discovery of fractals in 1967, was such a breakthrough in the Mathematics. In one of his quotes he says, "Nobody will deny that there is at least some roughness everywhere", and this was an open door for understanding the complexity of nature. Mandelbrot's new discovery of fractals led many earth scientists to take on his fractal approach another step forward and adopt it in measuring previous occurrences and making predictions about natural disasters in the future. For example, fractals were used to estimate and find order in systems like the shape of the British coastline (Lorditch, 2002).

From then scientists have used fractals in several areas of ecology. This is also because they are simple to generate on computers and are suitable in simulating natural phenomenon as proposed by Stanger (2006).

Fractal landscapes are computer generated figures that look like natural landscapes. They are composed of patterns that repeat themselves over a variety of scales. They are defined by two following important characteristics;

- Self similarity, means that part of an object will look similar to the whole if reduced or enlarged to the proper scales. For example, when you zoom in several times, you will observe the exact shape at every step. According to Mandelbrot (1983), the shape of a self similar object repeats itself with decrease or increase in the grain of measurement. This is known as statistical self-similarity and it implies that a fractal relationship found in nature will not remain the same across all scales but will only apply to a particular range of scales Mandelbrot (1983).

- Fractal Dimension given that a fractal must have a dimension that is not an integer (Halley *et al.*, 2004). This means that the dimensions are not always specific natural or whole numbers as seen in euclidean space where a point, a line, a polygon and a volume have a dimension of zero, one (length), two (length and width), and three (length, width and height) respectively, but lie in between giving us fractional dimensions. This explains the name fractal too.

Uses of fractal landscapes in ecology

Fractal landscapes are useful in explaining ecological systems. They provide a common ground for ecologists on whether to study the ecosystem as a whole or to consider it in parts. This can act as a connection between different areas in ecology.

Fractals are used to forecast calamities in nature including earthquakes, volcanic eruptions, landslides, hurricanes, wildfires, breakouts and floods. It is possible for predictions on size, location and timing of natural calamities and disasters to be done by observing the fractal arrangement and scale in which the patterns of chaos appear (Lorditch, 2002).

Fields like community ecology, population ecology and landscape ecology have applied fractal geometry in studying the movement of organisms and understanding the structure of a landscape (Ruis, 2000). This has provided insight in explaining the link between landscape and population structures.

The application of fractal geometry has provided understanding on the movement routes of animals since the movement of animals is not random, but rather it is determined by the fractal part of a landscape (Gautestad and Mysterud, 1993). These routes tend to be distorted as the environment gets complex.

Fractal dimensions eased the work of Ecologists by allowing them to model how roots grow in plants. The use of fractal patterns in root systems has led to an improvement in root growth models. In addition to the fact that root systems themselves are fractals by nature (Gautestad and Mysterud, 1993).

Landscape ecologists have gained a deep understanding of landscape structures. Looking at most ecosystems, they show patterns which are dependant on scales. This means that we can obtain information about the spatial structure and use this data to make conclusions on the spatial structure of the environment (Opdam *et al.*, 2001).

When there is variation of the patterns, the landscape is no longer homogeneous but rather heterogeneous. SA is one of the ways to show the presence of heterogeneity in a landscape (F Dormann *et al.*, 2007). This heterogeneity can be explained as positive, negative or zero SA. SA is observed in the change in spatial scales and this can be examined using fractals since they tell us more about the different spatial scales. Fractal landscapes generated with negative SA appear more fragmented than fractal landscapes with a positive SA.

Examples of fractals include the patterns on a aloe-spiral, the clouds in the air, the branching system of leaves and trees, crystals, mountain ranges, the branching system of a river and shorelines among others. Small tributaries join forming bigger and bigger "branches" in the system, and every small part of the system looks like the branching pattern as a whole (Lorditch, 2002).

Fractal methods are very effective for predicting and describing ecological patterns at several scales (Halley *et al.*, 2004). These methods are known as terrain generation methods and they have been used to create realistic landscapes as explained by Stanger (2006). They include the midpoint displacement method which was modified to the diamond square algorithm, generation using Fourier transform and multi fractal methods among others. We provide a brief explanation of how each method works in the following sections.

2.6 Methods used to generate fractal landscapes

2.6.1 Fourier transform method

The Fourier Transform method works with a non-repetitive process and starts with random Gaussian noise. Following Krista Bird (2013), the fast Fourier Transform (FFT) is applied to a two dimensional non-square grid of discrete random values. More specifically, the discrete Fourier transform is performed leading to a two dimensional discrete Fourier transform for the non-square grid.

The process starts when FFT decomposes the random noise into the sum of the sine and cosine functions and converts magnitudes into frequency(f) domain. Then the frequencies are scaled using a frequency filter of the form $\frac{1}{f^r}$, where f^r is the relative frequency. Thereafter an inverse FFT is applied so as to generate a fractal landscape by adding the sine and cosine waves at different frequencies. Terrain generation using FFT has an advantage of creating a fractal landscape with smooth rolling features rather than ridges and peaks (Krista Bird, 2013).

2.6.2 The multi fractal terrain generation

According to Stanger (2006), this is one of the latest method of them all, it uses images of real natural terrains to generate terrain with very accurate features. It generates a Levy noise field, filters the output of the first stage to get a multi scaling behaviour, then exponentiates and normalises the output obtained from stage two, and finally fractal integrates the multi fractal field (Stanger, 2006).

2.6.3 Midpoint displacement algorithm

This algorithm is straight forward, relatively easy to work with and produces realistic features. A line is drawn between two points then the midpoint of this line is displaced by some arbitrary positive random amount in a vertical direction. The midpoints of these two new line segments are then displaced by a random amount in the vertical direction. The process is repeated until a desired level of detail is reached ([Krista Bird, 2013](#)).

The challenge with this method is that it leaves square shaped artifacts in the terrain. According to [Krista Bird \(2013\)](#), attempts to solve this problem led to the diamond square algorithm, which deals with this by alternating calculated values to square and diamond patterned midpoints.

The midpoint displacement and the diamond square algorithm run in a linear time while as the Fourier transformation runs in non linear time ([Krista Bird, 2013](#)). For the purpose of this study we use the diamond square algorithm which we is described in chapter 3.

2.7 Summary

In this chapter, we have introduced and explained the concept of spatial scales and effects of scale on species distributions. We have also explained the concept of fractal landscape, and described methods for their generation and their spatial autocorrelation relationship.

Chapter 3

Model for generating and analysing fractal landscapes

In this chapter, we describe the model used to generate landscapes and analyse the data associated. We first explain in detail the diamond square, introduce the Integro Difference equation (IDE) by investigating species distributions through ecological processes of growth and dispersal. Thereafter, we illustrate the spatial temporal dynamics of the IDE on fractal landscapes, and finally, we introduce the statistical tools used to analyse data.

3.1 Diamond square method

There are several methods used to generate fractal landscapes as explained in chapter 2, however, in this section, we focus on the diamond square method. We take two fractal landscapes with known spatial and statistical properties on a 64 by 64 grid.

The landscapes define habitat types, where each grid cell can take on any numeric values. This allows exploration of properties of self similarity and the degree of spatial autocorrelation. The diamond square method generates a fractal landscape that represents a natural terrain. Each landscape represents a factor that affects species distribution. The main parameters used in the generation of the landscape are:

- Range, which is the fractal variation interval. It is represented as a random value between $[1, 10]$ in the fractal code in appendix A.
- A random value, h between 0 and 1 determining the roughness of the fractal. It is the factor by which the random deviations are reduced.
- The final matrix which is a square matrix of dimension 2^{n+1} where n is the number of iterations.

A step by step process is explained below

- Start with a two dimension array of size 2 by 2. The four corner points organised in the shape of a square of the array are assigned initial values, which can be either randomly chosen or predetermined. For this study, we use random values.
- In the diamond step, for each square in the array, we set the midpoint of that square to be the average of the four corner points plus a random value.
- In the square step, for each diamond in the array, we set the midpoint of that diamond to be the average of the four corner points plus a random value.
- The diamond and square steps are performed until all array values have been set.
- At every diamond and square step, the new range = Previous range (2^{-h}) as the process is repeated.
- In the square step, the points located at the edges of the array have only three adjacent values set instead of four. We solved by taking the fourth value from the other side of the array and wrap around (appearing as half sized diamonds) and thereafter calculate the center of diamonds. This method led us to a fractal landscape stitched together without discontinuities or breaks.

Figure 3.1 illustrates the diamond square algorithm.

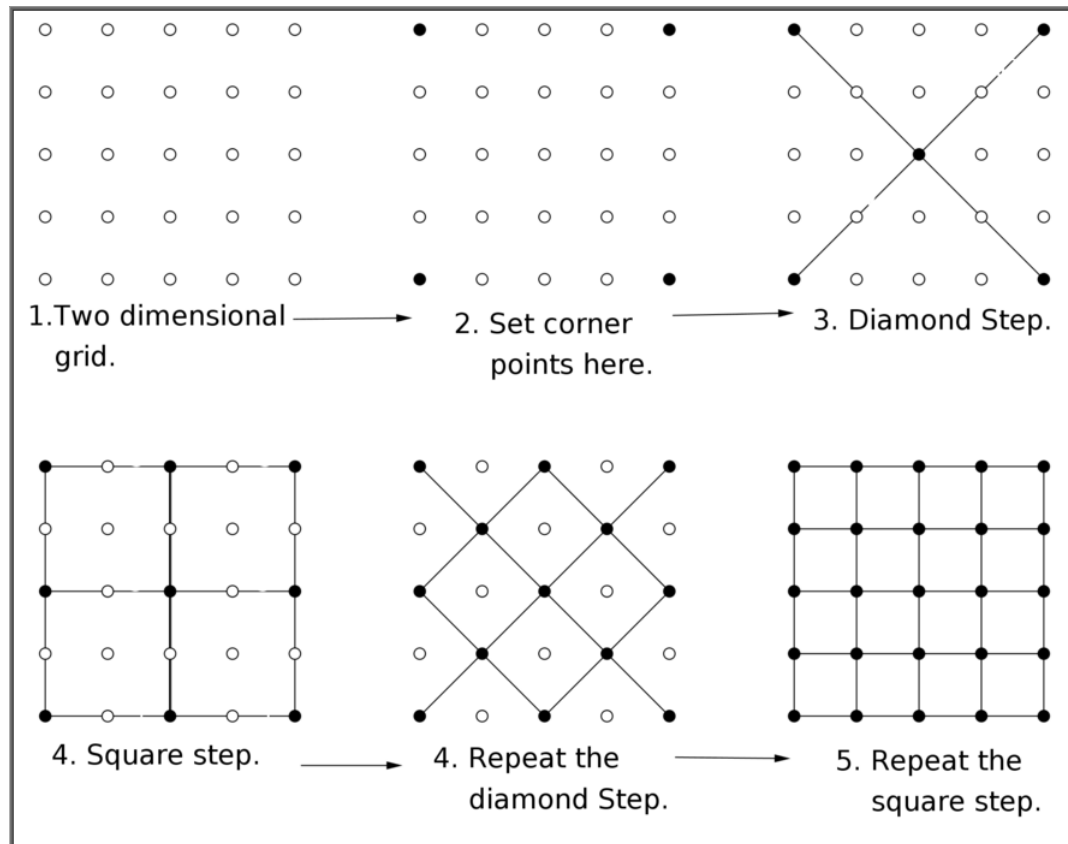


Figure 3.1: Six steps of the diamond square method

Figure 3.2 is an illustration of fractal landscapes in two dimensional(2D) when h (the smoothing parameter) is varied.

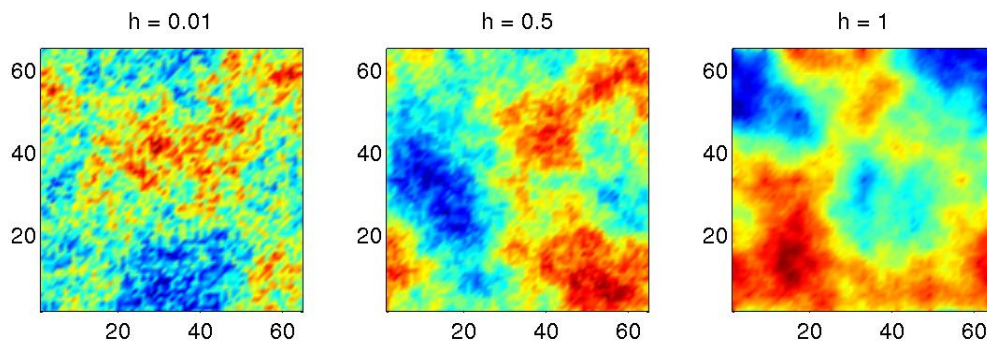


Figure 3.2: Fractal landscapes when $h = 0.01$, $h = 0.5$ and $h = 1$.

From Figure 3.2, we observe the different types of spatial autocorrelation. Fractal landscapes generated with negative spatial autocorrelation appear more fragmented than fractal landscapes with a positive spatial autocorrelation. For example when $h = 0.01$ we have negative spatial autocorrelation, $h = 0.5$ we have a random spatial autocorrelation, when $h = 1$ we have a positive spatial autocorrelation.

3.2 Integro difference equation (IDE)

Population dynamics through space are commonly modelled by reaction-diffusion equations, metapopulation equations and IDE.

According to Powell (2001), integro difference equations are spatial temporal models that describe reproduction, interaction and dispersal of species. They are continuous in space and discrete in time, and are popular for modelling growth and dispersal in biological populations. This explains why they are of interest to us in this project.

The behaviour of organisms in this model is represented as two phases of growth and dispersal since organisms can reproduce, interact and disperse. Diffusion models assume that these two phases occur at the same time. And when they do occur at discrete intervals then an IDE is more relevant for the formulation (Powell, 2001). Mathematically, an IDE is given as

$$N_{t+1}(x) = \int_{\Omega} k(x, y) f(N_t(y)) dy, \quad (3.2.1)$$

where

$N_t(x)$ is the population size at location x , at a time t ,

$k(x, y)$ is the dispersal kernel,

$f(N_t(y))$ is the population growth at location y ,

Ω is the domain in which x and y lie.

3.2.1 Growth stage

This is the stage of the population's behaviour that breeds to new population. This growth is based on the availability of resources and the capacity that the environment can hold (carrying capacity). There are several methods for modelling the growth rate with continuous and discrete time, density dependent and density independent. Examples of most commonly used density dependent models include the discrete logistic model, the Beverton-Holt Model, Gompertz Model and the Ricker model among others.

For this project, we used a Ricker logistic to model population of species in a habitat as proposed by [Gotelli and Gillman \(1996\)](#) in which the evolution of the population size over time is given by:

$$N_{t+1} = N_t e^{R \left(1 - \frac{N_t}{K}\right)}, \quad (3.2.2)$$

where

N is the population size at a time t ,

R is the population growth rate,

K is the carrying capacity,

N_{t+1} is the number of individuals in generation, at a time $(t + 1)$,

$(t + 1)$ is the time in the next generation.

Figure 3.3 illustrates the Ricker growth curve

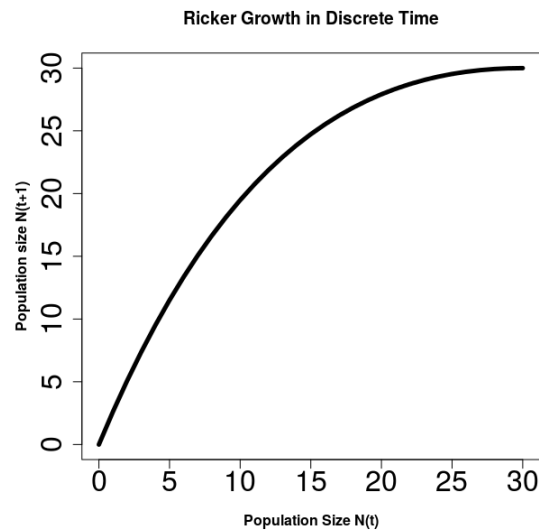


Figure 3.3: The Ricker growth curve with parameters $R = 1$ and $K = 10$;

3.2.2 Dispersal stage

Dispersal is the random movement of propagules settling into a substrate at a certain rate. Dispersal distance is characterised by individuals' movement in space which is described by a random process as individuals undergo a random-walk leading to diffusion from crowded patches to less-crowded adjacent patches (Liebhold *et al.*, 2004).

Powell (2001) defined a dispersal kernel as the probability distribution of the distance travelled by an individual from their natal site to a new place of potential establishment. The term dispersal kernel stems from mathematical studies of integro differential equations for population spread (Nathan *et al.*, 2012).

Selection of a dispersal distribution should be based on how well it fits the dispersal kernel as estimated from natural populations (Nathan *et al.*, 2012). Probability distributions like Gaussian, exponential are often used to describe dispersal kernels. They vary from one model to another and the tail fatness is dependant on the model parameters (Nathan *et al.*, 2012).

Dispersal has been modelled as a diffusion process with gaussian displacement although the dispersal kernels seen in several species are inclined to be more leptokurtic or fat tailed with a much higher probability of both short and long distance dispersal. Taking an example of plants, the shape of the dispersal kernel near the natal site is determined by the mechanism of dispersal. For instance, there may be a high peak near the origin for gravity or animal dispersal whereas there may be a minimum near the origin for wind dispersal (Furstenau and Cartwright, 2016).

Unlike diffusion equations, dispersal kernels enable us to include fine attributes of the movement patterns into a model. The shape of the dispersal

kernel influences population processes like the rate of population expansion, spatial distribution of species, local adaptation, responses to environmental dynamics, and speciation (Furstenau and Cartwright, 2016).

In this study we used a Gaussian dispersal kernel as it is thin tailed compared to the exponential kernel and the power law. More so it is adequate to represent the result of dispersal through diffusion so that we can predict the outcomes of dispersal using a random walk in a constant time.

To implement dispersal, we simulate the probabilistic dispersal of organisms using the Fast Fourier Transforms (FFT). We use FFT to evaluate the consequences of dispersal (Powell, 2001). Some of the variables we used to define space and the dispersal kernel are shown in Table 3.1.

Table 3.1: Descriptions of parameters and variables.

Parameter and variables	Description.
σ	Diffusion parameter.
t	Time.
x	Initial place of individual population.
y	Destination where population falls.
R	Instantaneous growth rate.
K	Carrying capacity.
N	Population density.
h_r	Smoothing factor for growth rate.
h_k	Smoothing factor for carrying capacity.

We illustrate how a population initially localised at a population disperses by computing the Gaussian dispersal kernel as follows.

$$k(x, y) = \frac{1}{\sqrt{4\pi\sigma^2}} \exp\left(-\frac{(x_1 - y_1)^2 + (x_2 - y_2)^2}{2\sigma^2}\right) \quad (3.2.3)$$

where $\in \mathbb{R}$ with $x = (x_1, x_2)$ and $y = (y_1, y_2)$ since we are working with 2D.

Dispersal as indicated from equation (3.2.1) is modelled by a Gaussian dispersal kernel, k in equation (3.2.3). Figure 3.4 illustrates a Gaussian kernel with parameters; distance from the source at point $(-8, 8)$ and probability distribution ranging from $(0.0, 0.4)$.

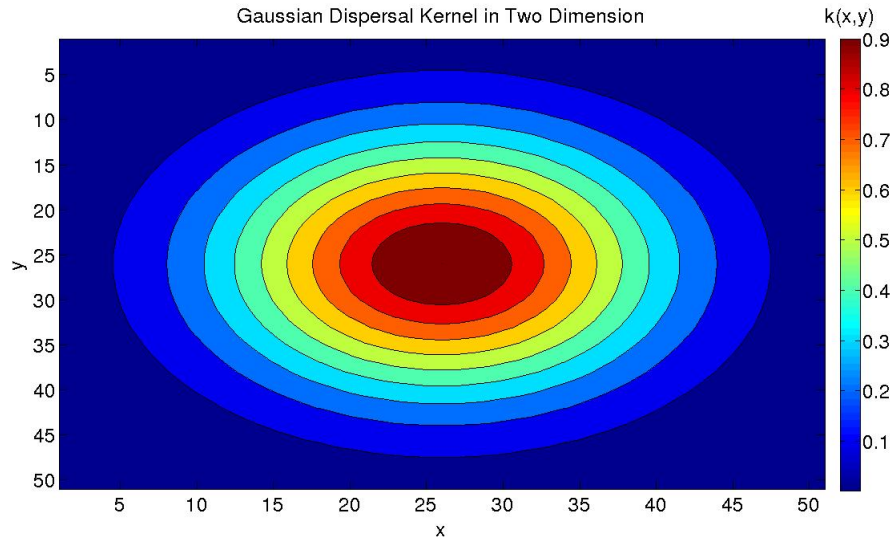


Figure 3.4: Gaussian dispersal kernel.

3.3 Spatial dynamics of the IDE on the landscape

In this section, we elaborate on the two fractal landscapes and how they change with time when applying the IDE. The simulations are run for 250 generations over 1000 times to enable us observe whether the parameters chosen randomly create a certain pattern after a very long time. This also caters for any cases of stochasticity in the model. We consider the following two cases:

- Case One: R and K are assigned numerical values in the range of $(-0.5, 1)$ and $(0.25, 1)$ respectively. Figure 3.5 shows the numerical simulation obtained. Figures 3.5 (a) and 3.5 (b) are fractal landscapes of R and K respectively. Figures 3.5 (c) – (f) shows us how the population increase over time until it stabilises. Figure 3.6 shows how the population changes after 250 generations and at randomly picked locations. The total population is dispersing on an increasing rate over time and this is because of the positive values of R .

In Figure 3.6 (g1), as the number of species in a habitat increase with time, reaches a point where species compete for resources and the habitat can no longer accommodate any increase and eventually, the population levels reaches a plateau at 2000.

In Figure 3.6 (g2), the individual population size at randomly chosen locations is increasing until 50 generations time when it stabilises. At some locations, the individual population sizes increases first for a short time and stabilises after 100 generations. The population size portrayed

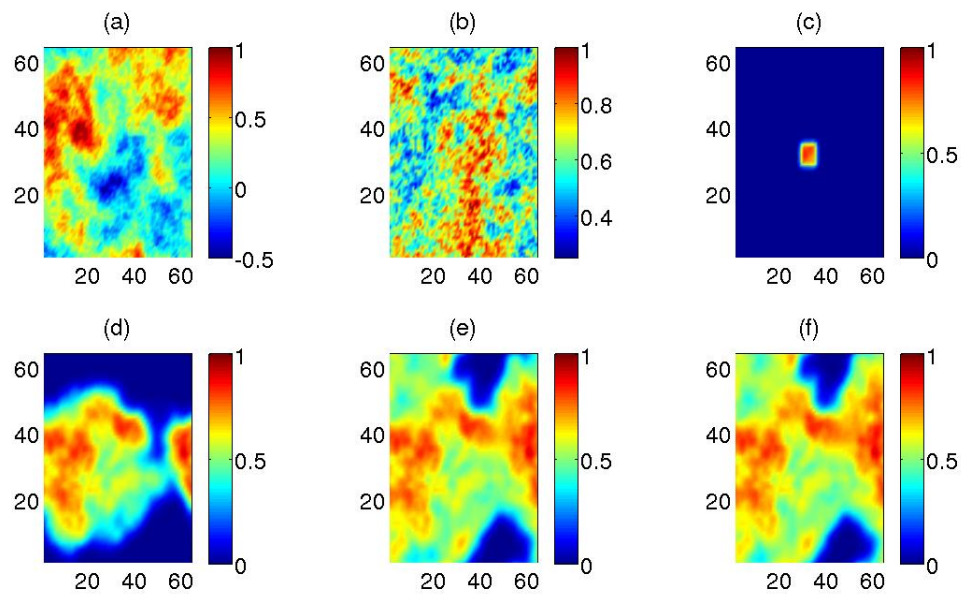


Figure 3.5: IDE on a fractal landscape for Time 1 to 250 .

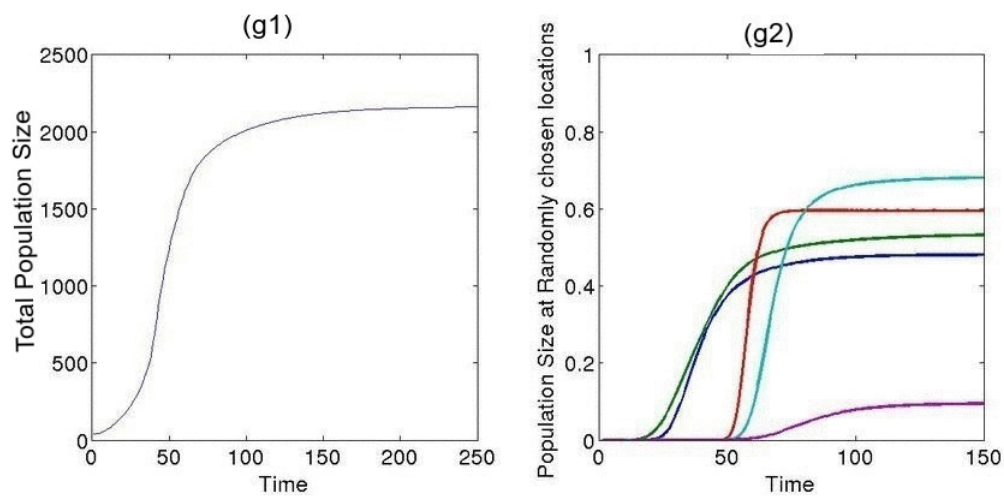


Figure 3.6: Population Size versus Time.

in Figure 3.6 ($g2$), is between 0 and 1 since it is population at individual locations.

- Case Two: R and K are assigned numerical values in the range of $[-0.5, 0.1]$ and $[0.01, 0.9]$ respectively. The value of h is changed where $h = 0.7$ for R and 0.5 for K .

Figure 3.7 is an illustration of the numerical simulations obtained. Figures 3.7 (A) and 3.7 (B) are fractal landscapes of R and K respectively. Figures 3.7 (C) and 3.7 (D) shows how population reduces over time.

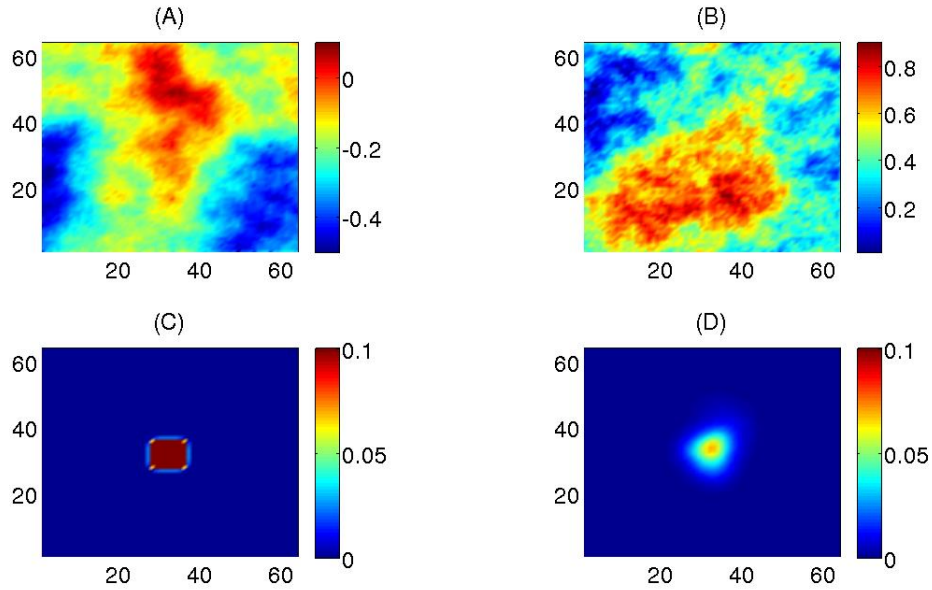


Figure 3.7: IDE on a fractal landscape for Time 1 to 50 .

Figure 3.8 shows how the total population changes after 50 generations and at randomly picked locations. The population is dispersing at a decreasing rate over time and this is because of the negative values of R .

In Figure 3.8 (E), the total number of species in a habitat decrease with increase in time. In Figure 3.8 (F), the individual population size at randomly chosen locations increases for less than 10 generations and decreases with increase in time. This is because when the growth rate is negative, the population will be affected negatively, hence the decrease.

In the Figure 3.8, although the population is not at zero, an extrapolation after along period of time shows that the population will go extinct.

This IDE model generated a standard population dataset. The simulation was performed in a 64 by 64 unit two-dimensional heterogeneous, square area with periodic boundaries to cater for the edge effect (differing biotic and abiotic conditions that exist at the boundaries due to contrasting environments in an ecosystem). The data sets were run for 250 generations and simulated over 1000 times. We obtained 3000 sets of data for the 3 matrices which we analysed using statistical methods of Hierarchical Partitioning (HP) and GLM.

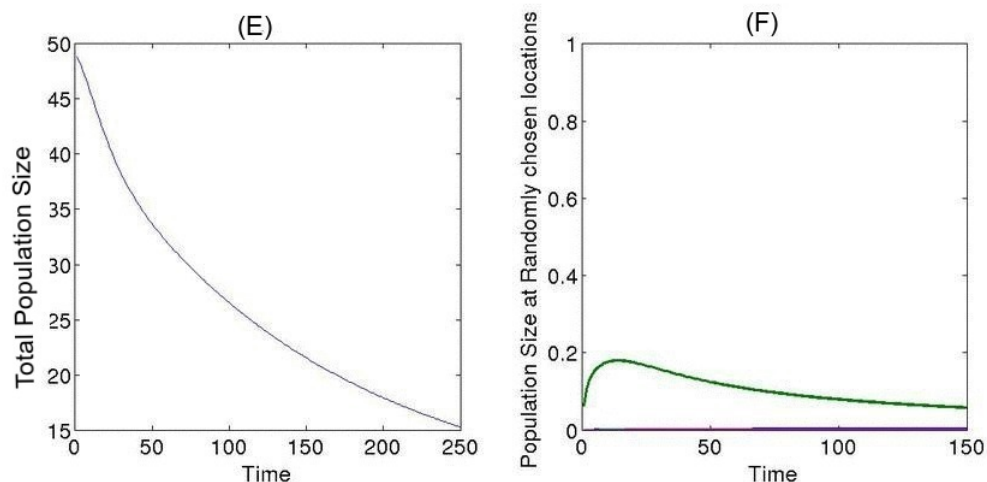


Figure 3.8: Population versus Time.

3.4 Statistical analysis of data generated

The focus in this section is to examine the relationship between growth rate, carrying capacity and population size using multiple regression preceded by the fractal dimension of data. Multiple regression is used by biologists and ecologists in identifying the factors that influence response variables. It is key is curbing multicollinearity hence reducing cases of generation of ambiguous results (Mac Nally, 2002). This is because the commonly used methods like linear regression may generate ambiguous results caused by the presence of multicollinearity (Mac Nally, 2002).

3.4.1 Fractal dimension (FD)

This is the measure of spatial heterogeneity in the environment, for example, in describing the spatial structures of species distribution (Li *et al.*, 2009). It permits us to measure the degree of complexity through evaluating how fast our measurements change as scale changes.

The box counting method analyses complex patterns by breaking the dataset into smaller pieces and examining the pieces at each smaller scale. By diminishing the size of the grid over time, we are able to accurately estimate the structure of the pattern.

Using the `fd.estim.boxcount` package in R, we calculate FD using the box counting method, which returns a numeric that does not exceed 2. We shall explore more in chapter 4.

3.4.2 Generalised linear model (GLM)

The GLM is an extension of the linear model that allows response variables to take on other probability distributions that are not necessarily normal distribution (Guisan *et al.*, 2002). The distribution of Y may be Gaussian, Binomial or Poisson. It is composed of a linear predictor (LP), which is the linear combination of predictor variables and is given by the equation:

$$\eta_i = \alpha + \beta_1 x_{i1} + \beta_2 x_{i2} + \cdots + \beta_p x_{ip};$$

(Guisan *et al.*, 2002) described the link and variance functions which are described below.

Link function (g) relating LP to the expected value of the response variable $\mu_i = E(Y_i)$. LP then becomes;

$$\eta_i = g(\mu_i).$$

Variance function describing how the variance (var) of Y depends on the mean μ giving,

$$\text{var}(Y_i) = \phi \text{var}(\mu),$$

where ϕ is the scale or dispersion parameter which is a constant.

According to Guisan *et al.* (2002), the advantages of a GLM over the traditional regression include:

1. No requirement of transforming Y to have a normal distribution.
2. More flexible since the choice of the link function is done independent of the response variables.
3. Ability to handle a larger class of distributions (exponential family distributions) for the response variable Y unlike in the linear model.
4. Easy implementation in the public domain software since it uses one procedure to capture all the models.

In this project, the GLM is fitted using the inbuilt function of "glm" which is of public domain in R.

3.4.3 Hierarchical partitioning (HP)

This is a method of multiple regression analysis that identifies the most likely casual factors while reducing multicollinearity (Olea *et al.*, 2010). Existence of collinearity is due to the complexity of ecological data and this is evident with correlation among explanatory variables. This becomes a challenge in

analysing the independent effects of the predictor variables to the response variable. HP presents joint and individual contribution of R and K to (N) . This is calculated using the public domain software package of "hier.part" in R.

3.5 Summary

In this chapter we have demonstrated the model used. We implemented an IDE on two fractal landscapes that were generated using the diamond algorithm. In IDE, the growth stage used the Ricker model and the dispersal stage used the Gaussian dispersal kernel. The model generated figures showing how the population changes with increase in time. Lastly we introduced the statistical methods that we will use in chapter 4 to analyse the data generated.

Chapter 4

Scale Resonance

4.1 Introduction

In this chapter, our main emphasis is analysis of the data obtained from the model explained in chapter 3. We do this using:

Sampling Effect to estimate the contribution of R and K to N and how these contributions vary as the sample size increases.

Scaling Effect to establish the contribution of R and K to N at different merged cells.

We evaluate these contributions using the Moran's I and fractal dimension of R and K , which influence N .

4.2 Sampling Effect

In this section, we randomly choose points from the data sets without replacement. For example 5, 10, 50, 100, 1000 were randomly selected for this project. "All Data" represents the entire data set before sampling is done.

4.2.1 The contribution of each variable

In this section, we take the growth rate (R) and carrying capacity(K) as independent variables. Using the inbuilt function of "hier.part" in R, we calculate the hierarchical partitioning of the data.

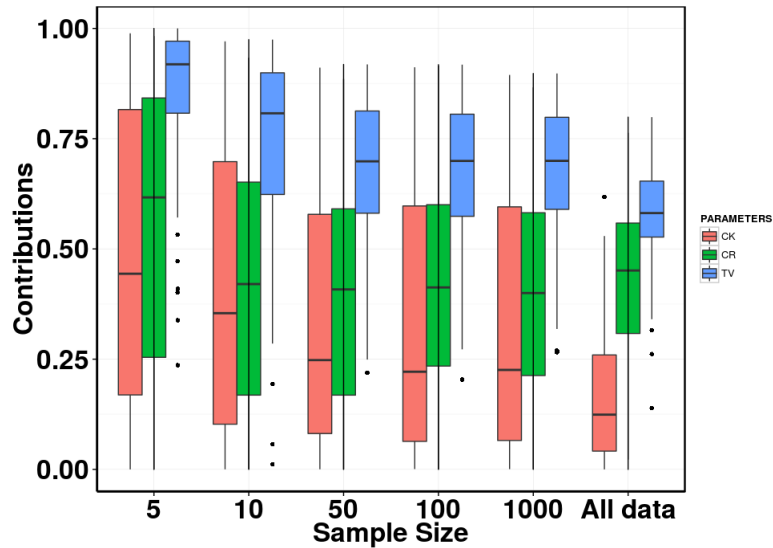


Figure 4.1: Contribution of R (CR) and K (CK) to N and total variance explained (R^2RK) at different sample size.

Figure 4.1 illustrates the total contribution of R and K to N , individual contribution of R to N and individual contribution of K to N as indicated in the blue, green and red box plots respectively.

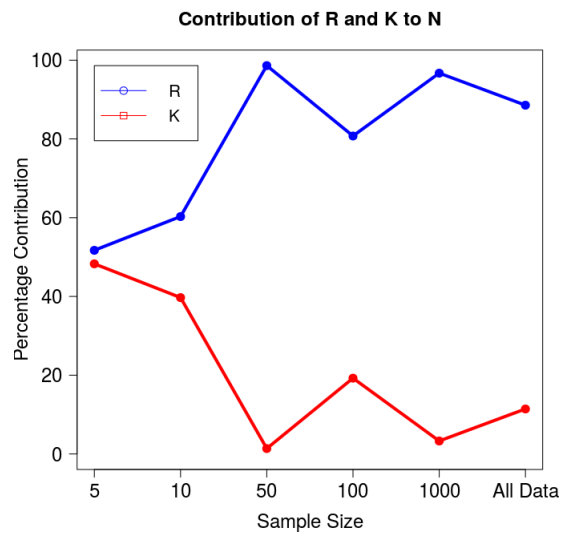


Figure 4.2: An example plot of the contributions of R and K as the function of the sample size.

Figure 4.2 shows how the contributions of each variable vary with the increase in sample size of one simulation. At the smallest sample, the contribu-

tion of R and K are equal i.e. 50%. As the sampled data points increase from 5 points to All Data, the percentage contribution of R increases as the one for K and vice versa. Growth rate (R), is predominating influencing population density, N , as sampled points are increased.

4.2.2 Spatial Autocorrelation of Sampled data.

Our concern here is to show how the spatial autocorrelation of N is affected by that of R and K . We calculate Moran's I of R (MR), K (MK) and N (MN) at randomly picked data points.

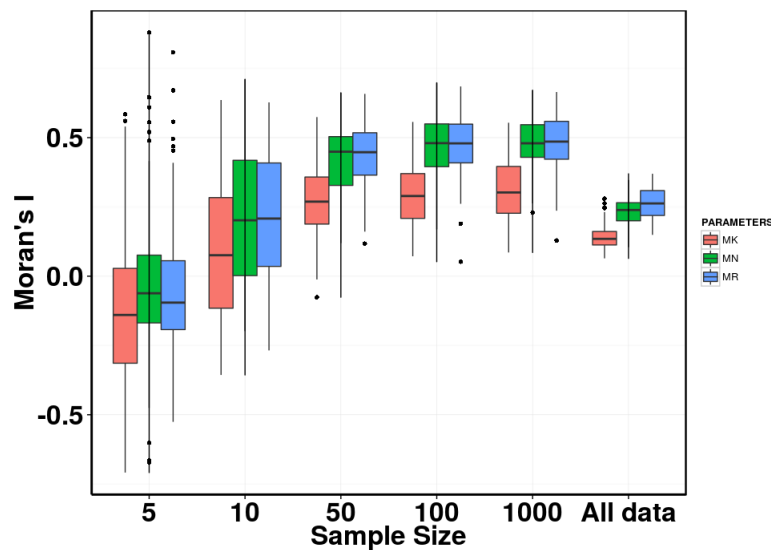


Figure 4.3: Moran's I of R (MR), K (MK) and N (MN) at different sample sizes.

Figure 4.3 shows the distribution of the Moran's I index. Moran's I of the three variables is increasing with increase in the sample size. The lowest Moran's I of the three variables is observed at sample size 5 and the highest when all the data points are chosen. K showed the lowest SA since its median from the quartile range is lower than the other two variables.

Sample sizes 5 and 10, showed the largest variability in the distributions of Moran's I of the three variables and include negative values. Negative SA exists at sample sizes 5 and 10 and becomes positive from sample size 50 and beyond.

4.2.2.1 Regression Coefficients

The coefficients in the table 4.1 describe the statistical relationship between MR , MK and MN .

Sample Size	Intercept	Coefficients of MR	Coefficients of MK
5	-0.00723	0.31275	0.33943
10	0.08865	0.51858	0.30833
50	0.1023	0.5188	0.4001
100	0.1532	0.4793	0.2990
1000	0.1802	0.4511	0.2730
All Data	0.1783	0.4529	0.2768

Table 4.1: Regression coefficients from MR , MK and MN at different sample sizes. Refer to RC1 in Figure 4.5.

In Table 4.1, the values of the coefficients reduce with increase in the sample sizes. The coefficients of MR at all sample sizes are greater than those of MK implying that a change in MR will lead to a greater change in MN . When MK is fixed, each change in MR at all sample sizes, MN changes.

All the regression coefficients are positive. For example, when the sample size is 100, a unit change in MR will increase MN by 0.4793, keeping MK constant. In this case, the model is given by $MN = 0.1532 + 0.4793MR + 0.2990MK$.

4.2.2.2 Statistical significance of regression model

We test the null hypothesis that MR and MK have no effect on MN . In the Table 4.2, the p-values of MR and MK are highly statistically significant since they are < 0.001 leading to the rejecting of the null hypothesis. This means that changes in MR and MK influence with changes in MN . The p-values of

Sample Size	p-values of intercept	p-values of MR	p-values of MK
5	0.777754	0.000319	0.000663
10	0.000895	8.07e-10	0.000532
50	0.0205	1.33e-09	2.83e-07
100	0.000990	1.44e-08	0.000315
1000	0.000130	4.82e-08	0.000333
All Data	0.000122	2.15e-08	0.000259

Table 4.2: p-values of MR , MK and MN at different sample sizes.

MR and MK covariates are < 0.05 , this means that the coefficients of MR and MK are all significant. They can potentially predict MN .

4.2.2.3 HP

To establish the influence of the two variables in explaining MN . Table 4.3 shows the individual and joint contributions. We notice that the independent contribution of MR is greater than that of MK for all sample sizes.

Sample Size	IR	IK	Joint RK
5	0.1361413	0.1238225	0.2339006
10	0.2970655	0.0822052	0.3792573
50	0.2263145	0.1381597	0.4112270
100	0.24320055	0.07712452	0.33844456
1000	0.22589520	0.07762717	0.32256232
All Data	0.23478671	0.07782717	0.33359546

Table 4.3: Joint and individual contributions at different sample sizes. Refer to HP1 in Figure 4.6.

4.2.3 Fractal Dimension

Figure 4.4 is an illustration of the distribution of Fractal dimensions. FDR, FDK and FDN are the fractal dimensions of R , K and N respectively.

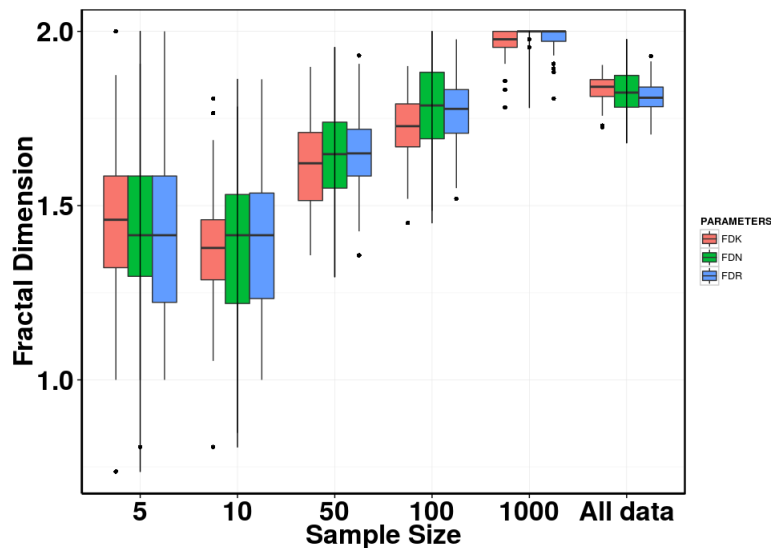


Figure 4.4: FDR, FDK and FDN at different sample sizes.

In Figure 4.4, the distribution of FDR, FDK and FDN as indicated in the blue, red and green box plots respectively.

4.2.3.1 Regression Coefficients

Table 4.4 shows how the fractal dimension of N is affected by the fractal dimensions of R and K as the sample size increases. In Table 4.4, the effects

Sample Size	Intercept	Coefficients of FDR	Coefficients of FDK
5	0.6740	0.2613	0.2908
10	0.2101	0.5632	0.2933
50	0.9620	0.1870	0.2305
100	0.7901	0.4444	0.1173
1000	1.83973	0.01322	0.06615
All Data	2.003083	-0.007689	0.005877

Table 4.4: Regression coefficients from the FDR and FDK at different sample sizes. Refer to RC2 in figure 4.5.

of changes of FDR and FDK on FDN alternate with increase in the sample size. For example, at sample size 50 when FDK is fixed, each change in one unit in FDR, FDN changes 0.2613 units and when FDR is fixed, each change in one unit in FDK, FDN changes 0.2908 units. The regression coefficients are positive except for All Data sample size. A unit change in FDR decreases the value of FDN by 0.007689 while keeping FDK constant. However, the regression coefficients for All Data and for sample size 1000 are not significant since p-values are > 0.05 . This suggests that the model becomes complex as the sample size is increased. It may be either over fitting or under fitting.

4.2.3.2 Statistical significance of regression coefficients

The p-values tell us whether to accept the null that the regression coefficients are zero or to reject the null that the regression coefficients are non zero. Results from Table 4.5 indicate that FDN is strongly dependant on FDR and

Sample size	p-values of intercept	p-values of FDR	p-values of FDK
5	0.01996	5.49e-06	0.00112
10	0.27594	7.19e-09	0.00435
50	0.000211	0.085816	0.051723
100	0.014798	0.000226	0.427895
1000	$<2e-16$	0.6757	0.0751
All Data	$<2e-16$	0.739	0.840

Table 4.5: p-values of FDR and FDK for different sample sizes.

FDK for sample sizes 5 and 10 since the p-values are < 0.05 . As the sample size increases, the FDK alone does not influence FDN as observed with p-values

> 0.05 . The p-value, 0.000226 indicates the FDN is dependant on FDR for at sample size 100.

4.2.3.3 HP

Table 4.6 indicates the joint contributions, individual contributions of FDR and FDK to FDN.

Sample Size	IR	IK	Joint RK
5	0.2235220	0.1384422	0.3044531
10	0.26556754	0.04497086	0.32492162
50	0.03373265	0.04204275	0.07089480
100	0.133200358	0.008505468	0.138827607
1000	0.0008833152	0.0313915309	0.0331463628
All Data	0.0011533171	0.0004255065	0.0015762843

Table 4.6: Joint and individual contributions of FDR and FDK at different sample sizes. Refer to HP2 in Figure 4.6.

Figure 4.5 is an illustration of the regression coefficients for sampling effect.

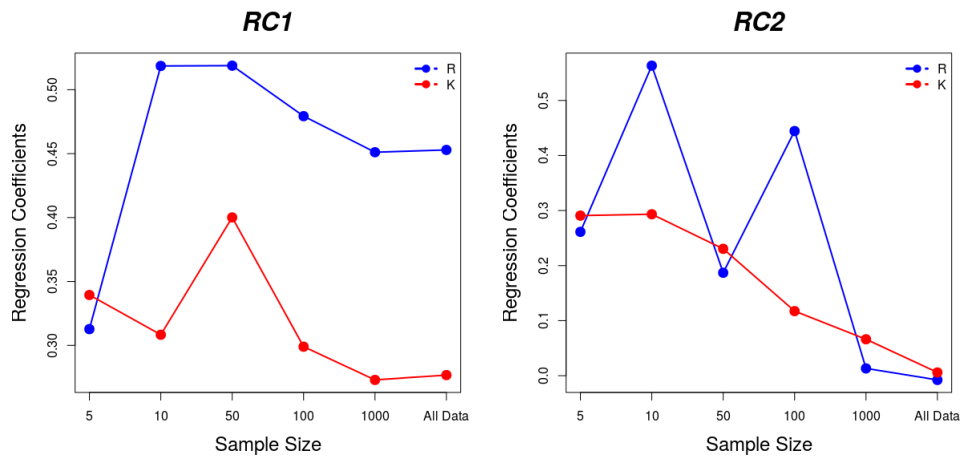


Figure 4.5: Regression coefficients of Moran's I (RC1) and FD (RC2) at different sample sizes.

Figure 4.6 is an illustration of HP for sampling effect.

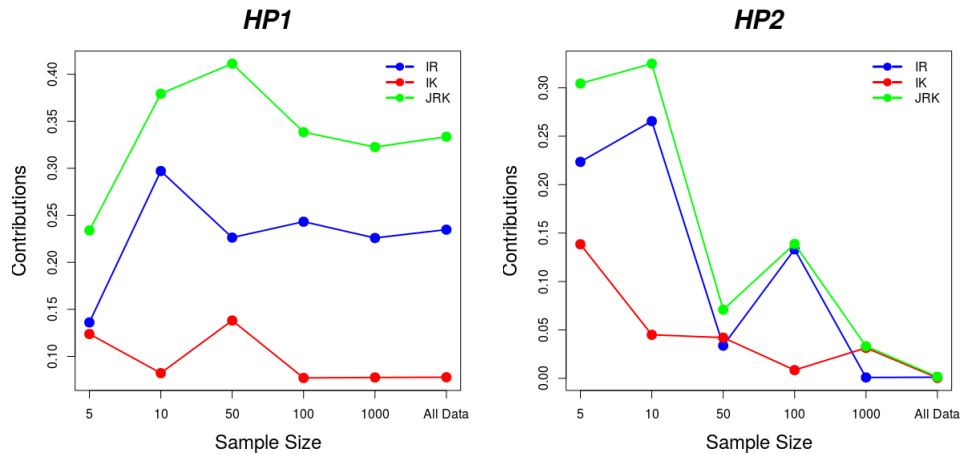


Figure 4.6: Contributions of Moran's I (HP1) and FD (HP2) at different sample sizes

4.3 Scaling Effect

In this section, we establish the relative effects of predictors when the grain size is changed. Scaling is done by merging grids together. The merging process is done using the following steps:

1. Take a 64 by 64 matrix.
2. Diminish the matrix using the mean of the grids.
3. Aggregate the matrix into 2 by 2, 4 by 4, 8 by 8 and 16 by 16 matrices.

In Figure 4.7, the total contribution, individual contributions of R and K increases with reduction in grid sizes up to grid 8. Thereafter, we observe a fall in the overall contributions.

4.3.1 Contribution of each variable at different merged grids.

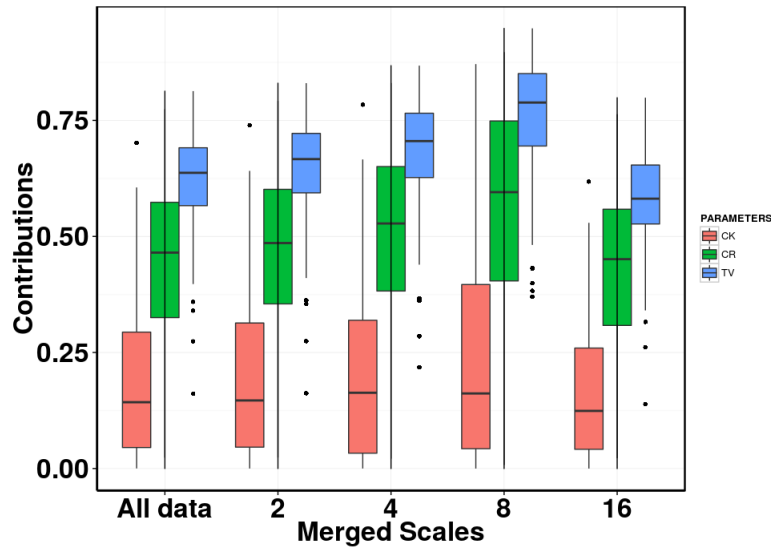


Figure 4.7: Contribution of R (CR) and K (CK) to N and total variance explained (TV) at different merged grids.

Figure 4.8 shows how the contributions of each variable vary when the grids are merged for one simulation.

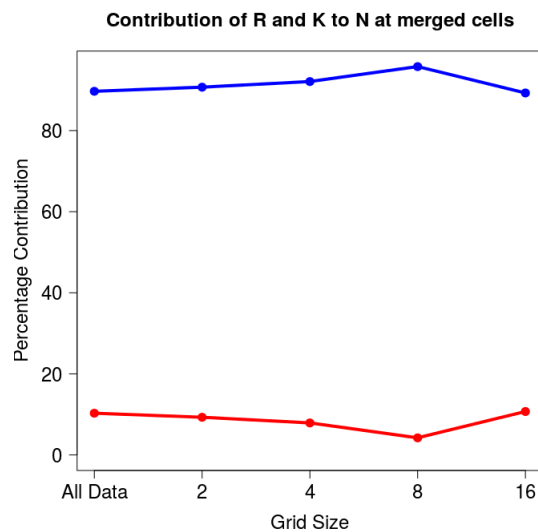


Figure 4.8: An example plot of the contributions of R and K as function of the merged grids. Blue and red correspond to R and K respectively.

4.3.2 Spatial Autocorrelation at different merged grids.

Figure 4.9 illustrates the distribution of Moran's I when the grids are merged.

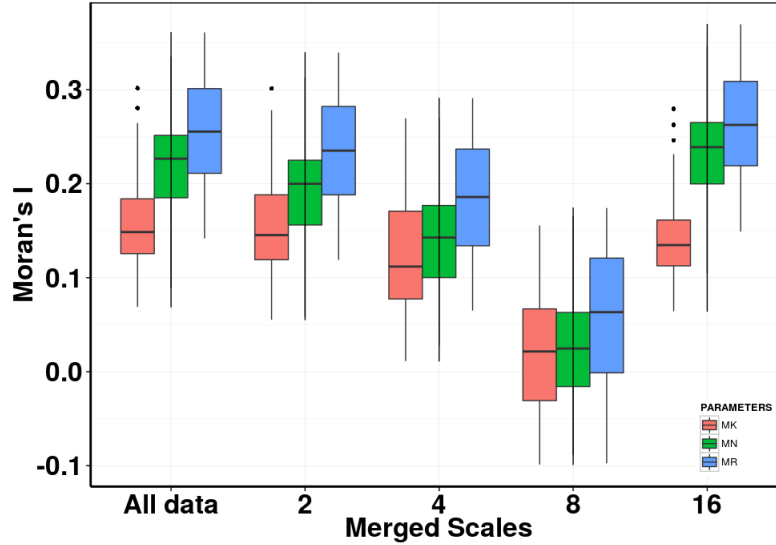


Figure 4.9: MR, MK and MN as functions of merged grids.

R has the highest Moran's I and variability of the range. The Moran's I of all the variables decreases until merged grid 8 and increases again at merged grid 16. Positive SA exists for all merged grids except at 8 by 8. Variables K and N have negative SA for merged grid 8 by 8.

4.3.2.1 Regression coefficients

Grid Size	Intercept	Coefficients of MR	Coefficients of MK
All Data	0.08068	0.50129	0.16630
$M_{2 \times 2}$	0.0692	0.5064	0.1496
$M_{4 \times 4}$	0.05732	0.50723	0.12732
$M_{8 \times 8}$	0.04057	0.49077	0.10041
$M_{16 \times 16}$	-6.794e-06	4.265e-01	6.337e-02

Table 4.7: Regression coefficients from MR and MK for different merged grids. Refer to RC3 in Figure 4.11

Table 4.7, keeping MK fixed, a small change in MR will affect MN greatly than when MR is fixed. Regression coefficients reduce as merged grid sizes increase. All the regression coefficients are positive and reduce as the merges increasing.

4.3.2.2 Statistical significance of regression coefficients

Grid size	p-values of intercept	p-values of MR	p-values of MK
All Data	0.000146	6.9e-11	0.067045
$M_{2 \times 2}$	0.00104	8.34e-11	0.07839
$M_{4 \times 4}$	0.00346	1.42e-10	0.11668
$M_{8 \times 8}$	0.00906	5.75e-10	0.19237
$M_{16 \times 16}$	0.999	8.61e-08	0.422

Table 4.8: p-values of MR and MK for different merged grids.

The p-values of R are < 0.05 leading to rejection of the null hypothesis. Moran's I of R is statistically significant and influences the Moran's I of N . At all merged scales, the p-values of $MR < 0.05$. This means that we reject the null that the regression coefficients are zero.

The p-values are increasing with an increase in the grid size. However, it is insignificant for the regression coefficients of MK . Since the p-values of MK coefficients are > 0.05 .

4.3.2.3 Hierarchical partitioning (HP)

Grid size	IR	IK	JointRK
All Data	0.37632600	0.06394677	0.39762922
$M_{2 \times 2}$	0.37386903	0.06136141	0.39364970
$M_{4 \times 4}$	0.36718236	0.05531121	0.38311810
$M_{8 \times 8}$	0.34732929	0.04533743	0.35872181
$M_{16 \times 16}$	0.26537915	0.01793593	0.27027806

Table 4.9: Joint and individual contributions of MR , MK and MN for different merged grids. Refer to HP3 in Figure 4.12.

Results in Table 4.9 show that contributions reduce with increase in the merges and also contributions of MR are greater than those of MK .

4.3.3 Fractal dimension at different merged grids.

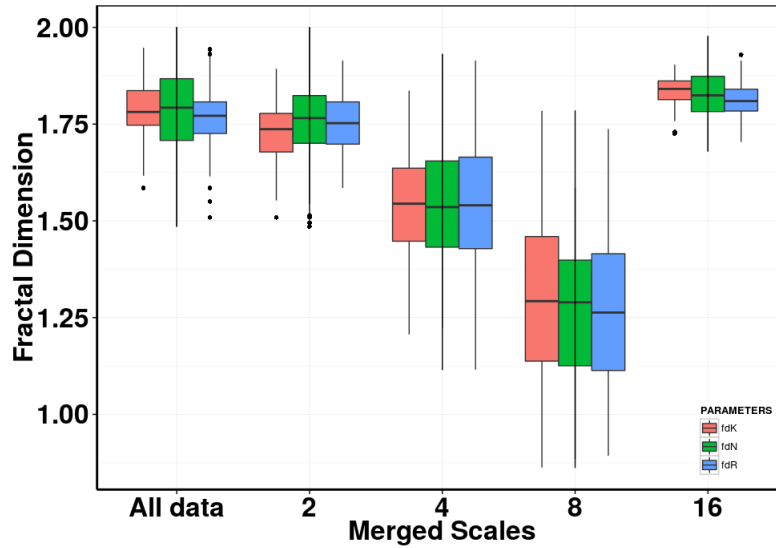


Figure 4.10: FDR, FDK and FDN for different merged grids.

In Figure 4.10, FD decreases with decrease in merged scales up to merge 8 and increase at 16. Merge 8 has the highest range variation for FDR, FDK and FDN. This means that as the matrix is merged to small sizes, the amount of complexity in the structure of patterns reduces.

4.3.3.1 Regression Coefficients

Grid Size	Intercept	Coefficients of FDR	Coefficients of FDK
All Data	1.5056	0.1030	0.1195
$M_{2 \times 2}$	1.2520	0.1124	0.2591
$M_{4 \times 4}$	2.07439	0.04518	0.03714
$M_{8 \times 8}$	0.5347	0.3496	0.4205
$M_{16 \times 16}$	0.6857	0.4513	0.2998

Table 4.10: FDR, FDK and FDN for different merged grids. Refer to RC4 in Figure 4.11.

In Table 4.10, the regression coefficients of FDR and FDK become significant when the grid size of the data is reduced for example $M_{8 \times 8}$ and $M_{16 \times 16}$.

Grid size	p-values of intercept	p-values of FDR	p-values of FDK
All Data	0.0154	0.4120	0.5223
$M_{2 \times 2}$	0.0351	0.5256	0.1345
$M_{4 \times 4}$	4.54e-14	0.567	0.627
$M_{8 \times 8}$	0.10157	0.00223	5.92e-06
$M_{16 \times 16}$	0.042675	4.92e-06	0.000586

Table 4.11: p-values of FDR and FDK at different merged grids.

4.3.3.2 Statistical significance of regression coefficients

The p-values at merged grids $M_{8 \times 8}$ and $M_{16 \times 16}$ are statistically significant for the FDR and FDK. This indicates that, at small scale, FDR and FDK have no influence on FDN.

4.3.3.3 Hierarchical partitioning (HP)

Grid Size	IR	IK	Joint RK
All Data	0.006256954	0.003537889	0.010464245
$M_{2 \times 2}$	0.004959225	0.023718766	0.027785327
$M_{4 \times 4}$	0.003842924	0.039017843	0.041363027
$M_{8 \times 8}$	0.09601043	0.19474154	0.26910229
$M_{16 \times 16}$	0.15999047	0.07741603	0.25681124

Table 4.12: Joint and individual contributions from FDR and FDK for merged grids. Refer to HP4 in Figure 4.12

The contribution of FD of K is greater than that of R up to merged grids of 4, and thereafter the contribution of the FDR is greater. The contributions are increasing up to the merged grid 8 and they drop at the merged grid 16. Figure 4.11 is an illustration of the regression coefficients for scaling effect.

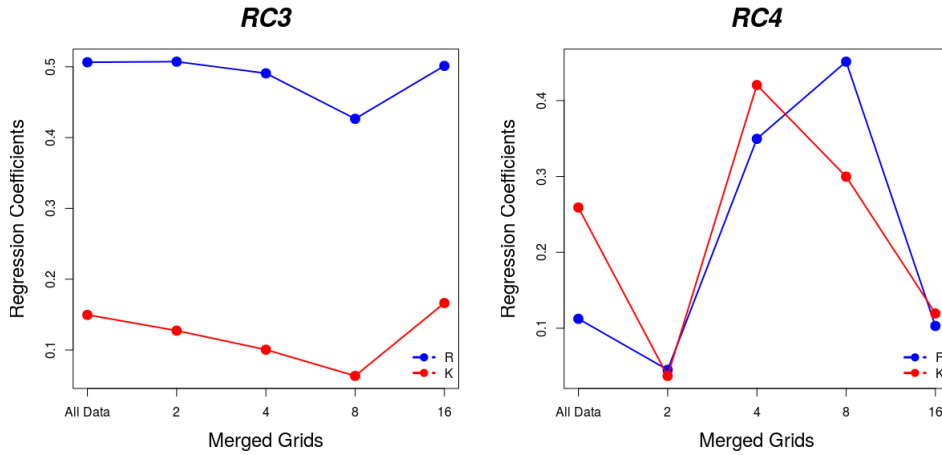


Figure 4.11: Regression coefficients of Moran's I (RC3) and FD (RC4) for different merged grids.

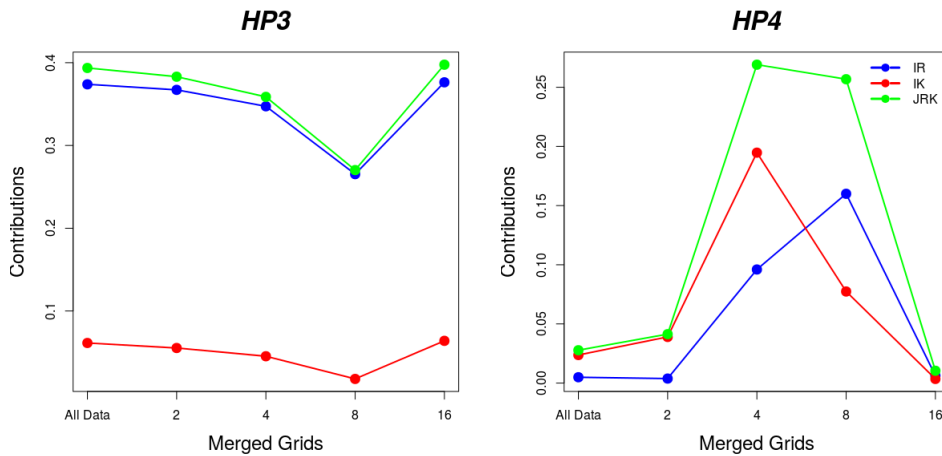


Figure 4.12: Contributions of Moran's I and FD for different merged grids.

4.4 Summary

We have looked at the sampling and scaling effect of R , K on N . In particular, we have analysed:

- the contribution of R , K on N ,
- how the SA of R and K influences the SA of N and
- how the FD of R and K influences the FD of N ,

Consequently we have calculated the regression coefficients, p-values and the hierarchical partitioning at every step. The regression coefficients of Moran's I and fractal dimension calculated from sampling and scaling effect as elaborated in Figure 4.5 and 4.11 show that R is more positively correlated to N than K is.

The two factors R and K can be thought of as key variables in determining population size. Using the results obtained in Tables 4.1, 4.2, 4.3, 4.4, 4.5 and 4.6, we conclude that as the sample sizes increase, variable R 's contribution is of key concern to population size.

In any habitat, a high growth rate (R) causes a population to reach its carrying capacity (K). In this thesis, results shown in Tables 4.7, 4.8, 4.9, 4.10, 4.11, 4.12 confirm that as the scale at which a population is measured increases, R becomes a more reliable factor in explaining N than its counter part K .

Chapter 5

Conclusion

Species distributions is the way in which species are arranged in space. Biogeographers have for long tried to examine the factors that drive this arrangement. Each species have a pattern of distribution that changes with the scale on which it is viewed. In this thesis, two factors that affect species distributions have been discussed; growth rate and carrying capacity. We evaluate their individual and joint contributions to population size.

Due to increased interest in species distribution modelling, I worked with a model that uses an integro difference equation to explain distribution of species. Simulation results give us a good picture of the changes in population size with increase in time. This means that there are more suitable habitats for species occupation as more time elapses. This model tells us that after along time, extinction happens when the growth rate, R takes on negative values as shown in Figure 3.8. In addition, numerical simulations show that the contribution of each variable is strongly affected by spatial heterogeneity in the variable.

In ecological literature, no explanation has been made on the term "scale resonance". This thesis has analysed the effect of changing spatial scales on two factors affecting species distribution. Results obtained revealed that at each scale, both factors are influence species distribution, however, growth rate is more influential at all scales.

I used fractal landscapes as a representation of each factor and analyse the change at local, regional and large scales. In doing so, the abundance of species is represented by the points of the grid where occupancy of the grids changes over time as illustrated in chapter 3.

Spatial scales play a role in influencing ecological processes since most of ecological phenomena depend on them (Fortin *et al.*, 2002). In this thesis, as the scales increase from small to large, the contribution of variables of growth rate and carrying capacity reduces. At small sample points, the contribution of each variable changes with that of growth rate greater than carrying capacity. Although as the sample points are increased, the contribution of the two variables, remains constant.

5.1 Recommendations for further research

Our work is limited to a model with two independent predictor variables in understanding species distributions. This work can be extended to incorporate more than two variables in the future. For example, estimating how factors like topography, land size, precipitation, temperature, e.t.c contribute to population density.

Further research needs to be done using real data. The abundance data in this project was randomly generated. These data was sometimes prone to errors and may not practically represent the landscapes. To implement a robust model, it is important to use real quantitative data.

Appendices

Appendix A

Codes For Simulation of Data.

The operating system used here is Ubuntu 14.04.4 LTS. Release: 14.04 with a codename:trusty. The codes in this chapter were implemented with the programming language:

```
MATLAB Version 7.13.0.564 (R2011b)
MATLAB License Number: 161052
Operating System: Linux 4.2.0-42-generic #49~14.04.1-Ubuntu SMP
Wed Jun 29 20:22:11 UTC 2016 x86_64
Java VM Version: Java 1.6.0_17-b04 with Sun Microsystems Inc.
Java HotSpot(TM) 64-Bit Server VM mixed mode
```

A.1 Pseudo code for the generation of a fractal landscape.

```
When the corner values of the squares
is greater than zero {
Go through the array and perform the diamond
step for each square present.
Go through the array and perform the square
step for each diamond present.
Then reduce the random number range.
}
```

A.2 Implemented code for the generation of a fractal landscape.

```
function x = fractal(h, maxstep)
range= 1;
```

```

x = rand(2); % Initial 2 by 2 matrix.
for step=2:maxstep
    x = diamond_square_algorithm(x,range ,step ,maxstep);
    range = range*2(-h);
end
end
%The diamond square algorithmn
function y = diamond_square_algorithm(x,range ,step ,maxstep)
x = addborders(x);
y = enlarge(x);
y = centerofsquares(y,range ,step ,maxstep);
y = wrap(y);
y = centerofdiamonds(y,range ,step ,maxstep);
y = removeborders(y);

end

function y = addborders(x)
y = zeros(size(x)+2);
y(2:end-1,2:end-1)=x;
end

function y = enlarge(x)
n = size(x,1);
y = zeros(2*n-3,2*n-3);
for i=2:n-1
    for j=2:n-1
        y(2*i-2,2*j-2)=x(i , j);
    end
end
end
end

function y = centerofsquares(x,range ,step ,maxstep)
n=size(x,1);
y = x;
for i=3:2:n-2
    for j=3:2:n-2
        y(i , j) =(y(i-1,j-1)+y(i+1,j+1)+y(i+1,j-1)+y(i-1,j+1))*0.25+2*ra
        %showit(removeborders(y),step ,maxstep ,i ,n-2,'Square ');
    end
end
end
end

function y=wrap(x)

```

```

y = x;
y(:,1) = x(:,end-2);
y(:,end) = x(:,3);
y(1,:) = x(end-2,:);
y(end,:) = x(:,3);
end

function y = centerofdiamonds(x,range,step,maxstep)
n=size(x,1);
y = x;
for i=2:1:n-1
    for j=3-mod(i,2):2:n-1
        y(i,j) = (y(i-1,j)+y(i+1,j)+y(i,j-1)+y(i,j+1))*0.25+2*range*rand;
        showit(removeborders(y),step,maxstep,i,n-1,'Diamond');
    end
end
end

function y = removeborders(x)
y=x(2:end-1,2:end-1);
end

function showit(x,step,maxstep,scan,maxscan,phase)
y = (zeros(2^(maxstep-1)+1));
insertlocations = linspace(1,2^(maxstep-1)+1,2^(step-1)+1);
y(insertlocations,insertlocations)=x;
plot(212)
imagesc(y')
axis equal
axis off;colormap gray
title(sprintf('Fractal landscape','FontSize',20,step,maxstep,scan,maxscan));
pause(0.01)
end

```

Appendix B

Codes For Data Analysis.

The operating system used here is Ubuntu 14.04.4 LTS. Release: 14.04 with a codename:trusty.

B.1 Code implemented in generation of data (IDE);

```
MATLAB Version 7.13.0.564 (R2011b)
MATLAB License Number: 161052
Operating System: Linux 4.2.0-42-generic #49~14.04.1-Ubuntu SMP
Wed Jun 29 20:22:11 UTC 2016 x86_64
Java VM Version: Java 1.6.0_17-b04 with Sun Microsystems Inc.
Java HotSpot(TM) 64-Bit Server VM mixed mode
```

```
Numsim =1001; %Number of simulations
```

```
%Landscape parameters.
```

```
maxstep = 7;
```

```
np = 2^(maxstep-1); %The size of the fractal landscape.
```

```
xl = 10; %Length of domain in x and y directions.
```

```
dx=2*xl/np; %Grid spacing.
```

```
x=linspace(-xl , xl-dx , np);
```

```
y = x;
```

```
[X,Y]=meshgrid(x,y);
```

```
%Time parameters.
```

```
ngens=200; % Number of generations.
```

```
dt = 1.0; %Time step length.
```

```
% Dispersal kernel
```

```
df=1.0; %diffusion coefficient.
```

```

%Gaussian movement kernel
hker = dx^2*exp(-(X.^2+Y.^2)/(2*df*dt))/(2*pi*dt*df);
Fhker=fft2(hker);

g = 1;
while g < Numsim
    h = rand;
    %For fractal k
    k0 = fractal(h, maxstep); %fractal one
    k=transformation(k0, 0.25, 1); %case one,
    k = k(1:end-1, 1:end-1);

    %For fractal r.
    h = rand;
    r0= fractal(h, maxstep); %fractal two.
    r=transformation(r0, -0.5, 1);
    r = r(1:end-1, 1:end-1);

    %Initiate population.
    p = zeros(np);
    origin = fix(np/2);
    p(origin-3:origin+3, origin-3:origin+3) = 1;
    for j=1:ngens
        hn=p.*exp(r.*(1-p./k)); %Ricker growth model
        fh=fft2(hn); %fft of the species.
        %The shift serves to center the probability functions.
        p = real(fftshift(iff2(Fhker.*fh)));
        maxpop = max(max(p));
        if isnan(maxpop)
            break;
        end
    end

    end
    if j == ngens
        % Write csv data sets here.
        fname = sprintf('valuesofR%d.csv', g);
        csvwrite(fname,r);
        fname = sprintf('valuesofK%d.csv', g);
        csvwrite(fname,k);
        fname = sprintf('valuesofN%d.csv', g);
        csvwrite(fname,p);
        g = g + 1;
    end
end
end

```

The details of the programming language used are explained as:

```
platform      x86_64-pc-linux-gnu
arch          x86_64
os            linux-gnu
system        x86_64, linux-gnu
status
major         3
minor         2.5
year          2016
month         04
day           14
svn rev       70478
language      R
version.string R version 3.2.5 (2016-04-14)
nickname      Very, Very Secure Dishes
```

B.2 Code for calculating the sampling effect

```
#Install the packages to use.
library("gtools")
library("hier.part")
library("abind")
library("ape")
library("fractaldim")
library("lattice")
library("reshape2")
library("reshape")
library("ggplot2")

#Function to calculate HP, Morans'I and FD of sampled data.
myfun <- function(popden, valuesofR, valuesofK, tmpdist){
  values = c()
  # HP
  independent <- data.frame(valuesofR, valuesofK)
  hierarchy <- hier.part(popden, independent,
    family="gaussian", gof="Rsqu", barplot=FALSE)
  values <- c(values, hierarchy$gfs[c(4, 2, 3)])

  # Morans' I
  values <- c(values, c(Moran.I(valuesofR, tmpdist)$observed))
  values <- c(values, c(Moran.I(valuesofK, tmpdist)$observed))
```

```

values <- c(values, c(Moran.I(popden, tmpdist)$observed))

# FD.
values <- c(values, fractaldim::fd.estim.boxcount(valuesofR)$fd)
values <- c(values, fractaldim::fd.estim.boxcount(valuesofK)$fd)
values <- c(values, fractaldim::fd.estim.boxcount(popden)$fd)

return(values)
}

#Read the datasets.
getdataSampling <- function(i){
  sampleddata <- c()
  valuesofR <- t(read.csv(paste0("valuesofR", i, ".csv"),
    header=FALSE, sep = ","))
  valuesofK <- t(read.csv(paste0("valuesofK", i, ".csv"),
    header=FALSE, sep = ","))
  popden <- t(read.csv(paste0("valuesofN", i, ".csv"),
    header=FALSE, sep = ","))

# Pick the samples points of 5, 10, 50, 100, 500, 1000, 4000
for(nsamples in c(5, 10, 50, 100, 500, 1000, 4000)){
  # Generate locations here
  locs <- sample(0:4095, nsamples, replace = FALSE)
  locx <- 1 + (locs %% 64)
  locy <- 1 + (locs %% 64)
  sampledR <- matrix(nrow = nsamples, ncol = 1)
  sampledK <- matrix(nrow = nsamples, ncol = 1)
  sampledN <- matrix(nrow = nsamples, ncol = 1)
  for (t in 1:nsamples){
    sampledR[t] = valuesofR[locx[t], locy[t]]
    sampledK[t] = valuesofK[locx[t], locy[t]]
    sampledN[t] = popden[locx[t], locy[t]]
  }

# Generate the distance matrix.
tmpdist = 1 / as.matrix(dist(cbind(locx, locy)))
diag(tmpdist) <- 0
tmpdist[is.infinite(tmpdist)] <- 0
sampleddata = rbind(sampleddata, myfun(as.vector(sampledN),
  as.vector(sampledR), as.vector(sampledK), tmpdist))
}
return(sampleddata)
}

```

```

# Initiate an empty list of the samples.
results.sample5 = c()
results.sample10 = c()
results.sample50 = c()
results.sample100 = c()
results.sample500 = c()
results.sample1000 = c()
results.sample4000 = c()

numsim = 100
for(i in 1:numsim){
  results = getdataSampling(i)
  results.sample5 = rbind(results.sample5, results[1,])
  results.sample10 = rbind(results.sample10, results[2,])
  results.sample50 = rbind(results.sample50, results[3,])
  results.sample100 = rbind(results.sample100, results[4,])
  results.sample500 = rbind(results.sample500, results[5,])
  results.sample1000 = rbind(results.sample1000, results[6,])
  results.sample4000 = rbind(results.sample4000, results[7,])
}

# Name the columns in the results of the sampled data.
colnames(results.sample5) <- c('R2_RK', 'R2_R', 'R2_K',
  'MoransR', 'MoransK', 'MoransN', 'fdR', 'fdK', 'fdN')
colnames(results.sample10) <- c('R2_RK', 'R2_R', 'R2_K',
  'MoransR', 'MoransK', 'MoransN', 'fdR', 'fdK', 'fdN')
colnames(results.sample50) <- c('R2_RK', 'R2_R', 'R2_K',
  'MoransR', 'MoransK', 'MoransN', 'fdR', 'fdK', 'fdN')
colnames(results.sample100) <- c('R2_RK', 'R2_R', 'R2_K',
  'MoransR', 'MoransK', 'MoransN', 'fdR', 'fdK', 'fdN')
colnames(results.sample500) <- c('R2_RK', 'R2_R', 'R2_K',
  'MoransR', 'MoransK', 'MoransN', 'fdR', 'fdK', 'fdN')
colnames(results.sample1000) <- c('R2_RK', 'R2_R', 'R2_K',
  'MoransR', 'MoransK', 'MoransN', 'fdR', 'fdK', 'fdN')
colnames(results.sample4000) <- c('R2_RK', 'R2_R', 'R2_K',
  'MoransR', 'MoransK', 'MoransN', 'fdR', 'fdK', 'fdN')

# Plot the Contribution of each variable here.
aK <- data.frame(results.sample5[,1], results.sample10[,1],
  results.sample50[,1], results.sample100[,1],
  results.sample1000[,1], results.sample4000[,1])
aN <- data.frame(results.sample5[,2], results.sample10[,2],
  results.sample50[,2], results.sample100[,2],

```



```
results.sample1000[,2], results.sample4000[,2])
aR <- data.frame(results.sample5[,3], results.sample10[,3],
  results.sample50[,3], results.sample100[,3],
  results.sample1000[,3], results.sample4000[,3])

# Plot Morans I here.
aR <- data.frame(results.sample5[,4], results.sample10[,4],
  results.sample50[,4], results.sample100[,4],
  results.sample1000[,4], results.sample4000[,4])
aK <- data.frame(results.sample5[,5], results.sample10[,5],
  results.sample50[,5], results.sample100[,5],
  results.sample1000[,5], results.sample4000[,5])
aN <- data.frame(results.sample5[,6], results.sample10[,6],
  results.sample50[,6], results.sample100[,6],
  results.sample1000[,6], results.sample4000[,6])

# Plot the Fractal dimension here
aR <- data.frame(results.sample5[,7], results.sample10[,7],
  results.sample50[,7], results.sample100[,7],
  results.sample1000[,7], results.sample4000[,7])
aK <- data.frame(results.sample5[,8], results.sample10[,8],
  results.sample50[,8], results.sample100[,8],
  results.sample1000[,8], results.sample4000[,8])
aN <- data.frame(results.sample5[,9], results.sample10[,9],
  results.sample50[,9], results.sample100[,9],
  results.sample1000[,9], results.sample4000[,9])

# Plot the Morans I of sampled adata here
a <- melt(aR)
head(a)
b <- c(5,10,50,100,1000)
aR1 <- aR
names(aR1) <- as.character(c(b," All data "))
head(aR1,2)
head(melt(aR1))
tail(melt(aR1))
aK1 <- aK
names(aK1) <- as.character(c(b," All data "))
aN1 <- aN
names(aN1) <- as.character(c(b," All data "))
a <- melt(aR1)
b <- melt(aK1)
c <- melt(aN1)
dim(a)
```

```

PARAMETERS <- rep(c("R2RK", "RR", "RK"), each=600)
head(PARAMETERS)
e <- rbind(a, c, b)
dim(e)
all.data <- data.frame(e, PARAMETERS)
head(all.data)
# Plot here.

ggplot(data = all.data, aes(x=variable, y=value))+
  geom_boxplot(aes(fill = PARAMETERS), width=1.0, main="Morans")+
  theme_bw()+ theme(axis.text=element_text(size=25, face="bold"),
  axis.title=element_text(size=25, face="bold"))+
  theme(axis.line=element_line(colour="black", size=1, linetype="solid"),
  panel.border = element_rect(colour = "black", fill=NA, size=1))+
  geom_line()+ labs(x="Sample Size", y="Contribution")+
  theme(plot.title = element_text(family = "Trebuchet MS",
  color="black", face="bold", size=32, hjust=0))

```

B.3 Code for calculating the scaling effect

```

Packages used.
library("gtools")
library("hier.part")
library("ape")
library("fractaldim")
library("lattice")
library("reshape")
library("MESS")

myfun <- function(popden, valuesofR, valuesofK, tmpdist){
  values = c()

# Hierarchical partitioning
  independent <- data.frame(as.vector(valuesofR),
  as.vector(valuesofK))
  hierarchy <- hier.part(as.vector(popden), independent,
  family="gaussian", gof="Rsqu", barplot=FALSE)
  values <- c(values, hierarchy$gfs[c(4, 2, 3)])

# Morans' I
  values <- c(values, c(Moran.I(as.vector(valuesofR), tmpdist)$observed))
  values <- c(values, c(Moran.I(as.vector(valuesofK), tmpdist)$observed))
  values <- c(values, c(Moran.I(as.vector(popden), tmpdist)$observed))

```

```

# Fractal dimension
values <-c(values , fractalDIM :: fd. estim. boxcount( valuesofR) $fd)
values <-c(values , fractalDIM :: fd. estim. boxcount( valuesofK) $fd)
values <-c(values , fractalDIM :: fd. estim. boxcount( popden) $fd)

return(values)
}

scaledata <- function(mm, ss){
  dd <- dim(mm)
  dx <- dd[1]
  dy <- dd[2]

  dscale = floor(dx / ss)
  tmpmat <- matrix(0, dscale, dscale)
  for (i in 0:(dscale-1)){
    for (j in 0:(dscale-1)){
      tmpmat[i+1,j+1]=mean(mm[(i*ss+1):((i+1)*ss) ,(j*ss+1):((j+1)*ss) ])
    }
  }
  return(tmpmat)
}

getdataScales <-function(i){
  scaleddata <- c()
  valuesofR <-t(read.csv(paste0("valuesofR",i,".csv"),
  header=FALSE, sep = ","))
  valuesofK <-t(read.csv(paste0("valuesofK",i,".csv"),
  header=FALSE, sep = ","))
  popden <-t(read.csv(paste0("valuesofN",i,".csv"),
  header=FALSE, sep = ","))

  for (ss in c(2, 4, 8, 16)){
    mergedR =scaledata(valuesofR, ss)
    mergedK =scaledata(valuesofK, ss)
    mergedP =scaledata(popden, ss)
    np = floor(64/ss)
    tmpx = ss*rep(1:np, np)
    dim(tmpx)<-c(np, np)
    tmpdist = 1 / as.matrix(dist(cbind(as.vector(tmpx),
    as.vector(t(tmpx)))))
    diag(tmpdist) <- 0
    scaleddata=rbind(scaledata ,myfun(mergedP ,mergedR ,mergedK , tmpdist))
  }
}

```

```

np = 64
tmpx = rep(1:np, np)
dim(tmpx) <- c(np, np)
tmpdist = 1 / as.matrix(dist(cbind(as.vector(tmpx),
as.vector(t(tmpx)))))
diag(tmpdist) <- 0
scaleddata = rbind(scaleddata, myfun(popden,
valuesofR, valuesofK, tmpdist))

return(scaleddata)
}
results.rawdata <- c()
results.scale2 <- c()
results.scale4 <- c()
results.scale8 <- c()
results.scale16 <- c()

numsim = 100
for(i in 1:numsim){
  results = getdataScales(i)
  results.rawdata = rbind(results.rawdata, results[1,])
  results.scale2 = rbind(results.scale2, results[2,])
  results.scale4 = rbind(results.scale4, results[3,])
  results.scale8 = rbind(results.scale8, results[4,])
  results.scale16 = rbind(results.scale16, results[5,])
}
# Name the columns here.
colnames(results.rawdata) <- c('R2_RK', 'R2_R', 'R2_K',
'MoransR', 'MoransK', 'MoransN', 'fdR', 'fdK', 'fdN')
colnames(results.scale2) <- c('R2_RK', 'R2_R', 'R2_K',
'MoransR', 'MoransK', 'MoransN', 'fdR', 'fdK', 'fdN')
colnames(results.scale4) <- c('R2_RK', 'R2_R', 'R2_K',
'MoransR', 'MoransK', 'MoransN', 'fdR', 'fdK', 'fdN')
colnames(results.scale8) <- c('R2_RK', 'R2_R', 'R2_K',
'MoransR', 'MoransK', 'MoransN', 'fdR', 'fdK', 'fdN')
colnames(results.scale16) <- c('R2_RK', 'R2_R', 'R2_K',
'MoransR', 'MoransK', 'MoransN', 'fdR', 'fdK', 'fdN')

# Plot the Contribution of each variable here.
aR <- data.frame(results.rawdata[,1], results.scale2[,1],
results.scale4[,1], results.scale8[,1], results.scale16[,1])
aK <- data.frame(results.rawdata[,2], results.scale2[,2],
results.scale4[,2], results.scale8[,2], results.scale16[,2])

```

```

aN <- data.frame(results.rawdata[,3], results.scale2[,3],
  results.scale4[,3], results.scale8[,3], results.scale16[,3])

#Plot Morans I.
aR <- data.frame(results.rawdata[,4], results.scale2[,4],
  results.scale4[,4], results.scale8[,4], results.scale16[,4])
aK <- data.frame(results.rawdata[,5], results.scale2[,5],
  results.scale4[,5], results.scale8[,5], results.scale16[,5])
aN <- data.frame(results.rawdata[,6], results.scale2[,6],
  results.scale4[,6], results.scale8[,6], results.scale16[,6])

# Plot the Fractal dimension
aR <- data.frame(results.rawdata[,7], results.scale2[,7],
  results.scale4[,7], results.scale8[,7], results.scale16[,7])
aK <- data.frame(results.rawdata[,8], results.scale2[,8],
  results.scale4[,8], results.scale8[,8], results.scale16[,8])
aN <- data.frame(results.rawdata[,9], results.scale2[,9],
  results.scale4[,9], results.scale8[,9], results.scale16[,9])

# Plot the Morans I of sampled data here
a <- melt(aR)
head(a)
b <- c(2, 4, 8, 16)
aR1 <- aR
names(aR1) <- as.character(c("All data", b))
head(aR1, 2)
head(melt(aR1))
tail(melt(aR1))
aK1 <- aK
names(aK1) <- as.character(c("All data", b))
aN1 <- aN
names(aN1) <- as.character(c("All data", b))
a <- melt(aR1)
b <- melt(aK1)
c <- melt(aN1)
dim(a)

# Label Parameters used here.
PARAMETERS <- rep(c("TV", "CR", "CK"), each=500)
PARAMETERS <- rep(c("MR", "MK", "MN"), each=500)
PARAMETERS <- rep(c("fdR", "fdK", "fdN"), each=500)
head(PARAMETERS)
e <- rbind(a, b, c)
dim(e)

```

```

all.data <- data.frame(e,PARAMETERS)
head(all.data)

# Final plot here.
ggplot(data = all.data, aes(x=variable, y=value))+
  geom_boxplot(aes(fill = PARAMETERS), width=1.0, main="Morans")+
  theme_bw()+
  theme(legend.justification=c(1,0), legend.position = c(1,0))+
  theme(axis.text=element_text(size=25, face="bold"),
        axis.title=element_text(size=25, face="bold"))+
  theme(axis.line=element_line(colour="black", size=1, linetype="solid"),
        panel.border = element_rect(colour = "black", fill=NA, size=1))+
  geom_line() + labs(x="Merged Scales", y="Fractal Dimension")+
  theme(plot.title = element_text(family = "Trebuchet MS",
        color="black", face="bold", size=32, hjust=0))

# Perform a glm here for the samples
Regression Coefficients here.
MoransRall <- results.rawdata[,4]
MoransKall <- results.rawdata[,5]
MoransNall <- results.rawdata[,6]
mall=glm(MoransNall~MoransRall+MoransKall)
summary(mall)
hier.part(MoransNall, data.frame(MoransRall, MoransKall),
family="gaussian", gof="Rsqu", barplot=FALSE)

MoransR2 <- results.scale2[,4]
MoransK2 <- results.scale2[,5]
MoransN2 <- results.scale2[,6]
m2=glm(MoransN2~MoransR2+MoransK2)
summary(m2)
hier.part(MoransN2, data.frame(MoransR2, MoransK2),
family="gaussian", gof="Rsqu", barplot=FALSE)

MoransR4 <- results.scale4[,4]
MoransK4 <- results.scale4[,5]
MoransN4 <- results.scale4[,6]
m4=glm(MoransN4~MoransR4+MoransK4)
summary(m4)
hier.part(MoransN4, data.frame(MoransR4, MoransK4),
family="gaussian", gof="Rsqu", barplot=FALSE)

```

```

MoransR8 <- results.scale8[,4]
MoransK8 <- results.scale8[,5]
MoransN8 <- results.scale8[,6]
m8=glm(MoransN8~MoransR8+MoransK8)
summary(m8)
hier.part(MoransN8,data.frame(MoransR8, MoransK8),
family="gaussian", gof="Rsqu", barplot=FALSE)

```

```

MoransR16 <- results.scale16[,4]
MoransK16 <- results.scale16[,5]
MoransN16 <- results.scale16[,6]
m16=glm(MoransN16~MoransR16+MoransK16)
summary(m16)
hier.part(MoransN16,data.frame(MoransR16, MoransK16),
family="gaussian", gof="Rsqu", barplot=FALSE)

```

Perform a glm here for the samples.

Regression Coefficients here for fractal dimension

```

fdRall <- results.rawdata[,7]
fdKall <- results.rawdata[,8]
fdNall <- results.rawdata[,9]
fdall=glm(fdNall~fdRall+fdKall)
summary(fdall)
hier.part(fdNall,data.frame(fdRall, fdKall),
family="gaussian", gof="Rsqu", barplot=FALSE)

```

```

fdR2 <- results.scale2[,7]
fdK2 <- results.scale2[,8]
fdN2 <- results.scale2[,9]
fd2=glm(fdN2~fdR2+fdK2)
summary(fd2)
hier.part(fdN2,data.frame(fdR2, fdK2),
family="gaussian", gof="Rsqu", barplot=FALSE)

```

```

fdR4 <- results.scale4[,7]
fdK4 <- results.scale4[,8]
fdN4 <- results.scale4[,9]

```

```
fd4=glm(fdR4~fdK4+fdN4)
summary(fd4)
hier.part(fdN4,data.frame(fdR4, fdK4),
family="gaussian", gof="Rsqu", barplot=FALSE)
```

```
fdR8 <- results.scale8[,7]
fdK8 <- results.scale8[,8]
fdN8 <- results.scale8[,9]
fd8=glm(fdN8~fdR8+fdK8)
summary(fd8)
hier.part(fdN8,data.frame(fdR8, fdK8),
family="gaussian", gof="Rsqu", barplot=FALSE)
```

```
fdR16 <- results.scale16[,7]
fdK16 <- results.scale16[,8]
fdN16 <- results.scale16[,9]
fd16=glm(fdN16~fdR16+fdK16)
summary(fd16)
hier.part(fdN16,data.frame(fdR16, fdK16),
family="gaussian", gof="Rsqu", barplot=FALSE)
```


List of References

- Al-Hamdan, M., Cruise, J., Rickman, D. and Quattrochi, D. (2010). Effects of spatial and spectral resolutions on fractal dimensions in forested landscapes. *Remote Sensing*, vol. 2, no. 3, pp. 611–640.
- Amissah, L., Mohren, G.M., Bongers, F., Hawthorne, W.D. and Poorter, L. (2014). Rainfall and temperature affect tree species distribution in Ghana. *Journal of Tropical Ecology*, vol. 30, no. 05, pp. 435–446.
- Austin, M. (2007). Species distribution models and ecological theory: a critical assessment and some possible new approaches. *Ecological Modelling*, vol. 200, no. 1, pp. 1–19.
- Bjørnstad, O.N., Ims, R.A. and Lambin, X. (1999). Spatial population dynamics: analyzing patterns and processes of population synchrony. *Trends in Ecology & Evolution*, vol. 14, no. 11, pp. 427–432.
- Chave, J. (2013). The problem of pattern and scale in ecology: what have we learned in 20 years? *Ecology Letters*, vol. 16, no. s1, pp. 4–16.
- Chevalier, M., Laffaille, P. and Grenouillet, G. (2014). Spatial synchrony in stream fish populations: influence of species traits. *Ecography*, vol. 37, no. 10, pp. 960–968.
- Elith, J. and Leathwick, J.R. (2009). Species distribution models: ecological explanation and prediction across space and time. *Annual Review of Ecology, Evolution, and Systematics*, vol. 40, no. 1, p. 677.
- F Dormann, C., M McPherson, J., B Araújo, M., Bivand, R., Bolliger, J., Carl, G., G Davies, R., Hirzel, A., Jetz, W., Daniel Kissling, W. *et al.* (2007). Methods to account for spatial autocorrelation in the analysis of species distributional data: a review. *Ecography*, vol. 30, no. 5, pp. 609–628.
- Fortin, M.-J., Dale, M.R. and Ver Hoef, J.M. (2002). Spatial analysis in ecology. *Wiley StatsRef: Statistics Reference Online*, vol. 1, no. 1, pp. 1–9.
- Fournier, A., Fussell, D. and Carpenter, L. (1982). Computer rendering of stochastic models. *Communications of the ACM*, vol. 25, no. 6, pp. 371–384.
- Furstenau, T.N. and Cartwright, R.A. (2016). The effect of the dispersal kernel on isolation-by-distance in a continuous population. *PeerJ*, vol. 4, p. e1848.

- Gautestad, A.O. and Mysterud, I. (1993). Physical and biological mechanisms in animal movement processes. *Journal of Applied Ecology*, pp. 523–535.
- Gneiting, T., Ševčíková, H. and Percival, D.B. (2012). Estimators of fractal dimension: Assessing the roughness of time series and spatial data. *Statistical Science*, pp. 247–277.
- Gotelli, N.J. and Gillman, M. (1996). A primer of ecology. *Trends in Ecology and Evolution*, vol. 11, no. 6, pp. 264–265.
- Guisan, A., Edwards, T.C. and Hastie, T. (2002). Generalized linear and generalized additive models in studies of species distributions: setting the scene. *Ecological Modelling*, vol. 157, no. 2, pp. 89–100.
- Guisan, A., Graham, C.H., Elith, J. and Huettmann, F. (2007). Sensitivity of predictive species distribution models to change in grain size. *Diversity and Distributions*, vol. 13, no. 3, pp. 332–340.
- Halley, J., Hartley, S., Kallimanis, A., Kunin, W., Lennon, J. and Sgardelis, S. (2004). Uses and abuses of fractal methodology in ecology. *Ecology Letters*, vol. 7, no. 3, pp. 254–271.
- Henle, K., Potts, S., Kunin, W., Matsinos, Y., Simila, J., Pantis, J., Grobelnik, V., Penev, L. and Settele, J. (2014). Scaling in ecology and biodiversity conservation. *Advanced Books*, vol. 1, p. e1169.
- Hewitt, J.E., Thrush, S.F. and Lundquist, C. (2010). Scale-dependence in ecological systems. *Essential for Life Sciences*, vol. 1, no. 7, pp. 1–7.
- Hortal, J., Roura-Pascual, N., Sanders, N. and Rahbek, C. (2010). Understanding (insect) species distributions across spatial scales. *Ecography*, vol. 33, no. 1, p. 51.
- Jager, H.I. (ed.) (2007). *Scaling and uncertainty analysis in ecology: methods and applications*, pp. 267–268. Wiley Online Library, Oxford.
- Kamino, L.H., Stehmann, J.R., Amaral, S., De Marco, P., Rangel, T.F., de Siqueira, M.F., De Giovanni, R. and Hortal, J. (2012). Challenges and perspectives for species distribution modelling in the neotropics. *The Royal Society*, vol. 8, no. 10, pp. 324–326.
- Kendall, B.E., Bjørnstad, O.N., Bascompte, J., Keitt, T.H. and Fagan, W.F. (2000). Dispersal, environmental correlation, and spatial synchrony in population dynamics. *The American Naturalist*, vol. 155, no. 5, pp. 628–636.
- Koenig, W.D. (2002). Global patterns of environmental synchrony and the moran effect. *Ecography*, vol. 25, no. 3, pp. 283–288.
- Krista Bird, Thomas Dickerson, J.G. (2013). Techniques of fractal terrain generation methods. 4th April 2016.
Available at: http://web.williams.edu/Mathematics/sjmillier/public_html/hudson/Dickerson_Terrain.pdf

- Levin, A.S. (1992). The problem of pattern and scale in ecology. *Ecology*, vol. 73, no. 6, pp. 1943–1967.
- Li, J., Du, Q. and Sun, C. (2009). An improved box-counting method for image fractal dimension estimation. *Pattern Recognition*, vol. 42, no. 11, pp. 2460–2469.
- Liebhold, A., Koenig, W.D. and Bjørnstad, O.N. (2004). Spatial synchrony in population dynamics. *Annual Review of Ecology, Evolution, and Systematics*, pp. 467–490.
- Lorditch, E. (2002). Earth scientists use fractals to measure and predict natural disasters. *Inside Science News Service*.
- Mac Nally, R. (2002). Multiple regression and inference in ecology and conservation biology: further comments on identifying important predictor variables. *Biodiversity & Conservation*, vol. 11, no. 8, pp. 1397–1401.
- Mandelbrot, B.B. (1983). *The fractal geometry of nature*, vol. 173. Macmillan.
- McGarigal, K. (2016). Concepts of scale. Date accessed: 21 June 2016.
Available at: http://www.umass.edu/landeco/teaching/landscape_ecology/schedule/chapter2_scale.pdf
- McGill, B.J. *et al.* (2010). Matters of scale. *Science*, vol. 328, no. 5978, pp. 575–576.
- Moran, P.A. (1950). Notes on continuous stochastic phenomena. *Biometrika*, vol. 37, no. 1/2, pp. 17–23.
- Nathan, R., Klein, E., Robledo-Arnuncio, J.J. and Revilla, E. (2012). Dispersal kernels: review. *Dispersal Ecology and Evolution*. Oxford University Press. Oxford. pp, pp. 187–210.
- Olea, P.P., Mateo-Tomás, P. and De Frutos, Á. (2010). Estimating and modelling bias of the hierarchical partitioning public-domain software: implications in environmental management and conservation. *PLoS One*, vol. 5, no. 7, p. e11698.
- Opdam, P., Foppen, R. and Vos, C. (2001). Bridging the gap between ecology and spatial planning in landscape ecology. *Landscape Ecology*, vol. 16, no. 8, pp. 767–779.
- Paradis, E., Claude, J. and Strimmer, K. (2004). Ape: analyses of phylogenetics and evolution in r language. *Bioinformatics*, vol. 20, no. 2, pp. 289–290.
- Plate, T. and Heiberger, R. (2011). abind: Combine multi-dimensional arrays. *R package version*, pp. 1–3.
- Powell, J. (2001). Spatio-temporal models in ecology; an introduction to integro-difference equations. *Annual Review of Ecology, Evolution, and Systematics*, vol. 1, no. 1, pp. 1–42.
- Powell, T.M. and Steele, J.H. (2012). *Ecological time series*. Springer Science & Business Media.

- Richardson, D.M. and Pyšek, P. (2008). Fifty years of invasion ecology—the legacy of Charles Elton. *Diversity and Distributions*, vol. 14, no. 2, pp. 161–168.
- Robert, R. and Sokal, F. (1978). Spatial autocorrelation in biology. *Biological Journal of the Linnean Society*, vol. 10, pp. 199–228.
- Ruis, J. (2000). The application of fractal geometry to ecology. Date accessed: 10th February 2016.
Available at: <http://www.fractal.org/Bewustzijns-Besturings-Model/Application-Fractal-Geometry.pdf>
- Sarkar, D. (2008). *Lattice: multivariate data visualization with R*. Springer Science & Business Media.
- Sawada, M. (2004). Global spatial autocorrelation indices—Moran's I , Geary's C and the general cross-product statistic. *Research Paper from the Laboratory for Paleoclimatology and Climatology at the University of Ottawa*. (as posted online at: <http://www.lpc.uottawa.ca/publications/moransi/moran.htm>).
- Schneider, D.C. (2001). The rise of the concept of scale in ecology: the concept of scale is evolving from verbal expression to quantitative expression. *BioScience*, vol. 51, no. 7, pp. 545–553.
- Scott, A. *et al.* (2006). *Encyclopedia of nonlinear science*. Routledge.
- Sheppard, L.W., Bell, J.R., Harrington, R. and Reuman, D.C. (2015). Changes in large-scale climate alter spatial synchrony of aphid pests. *Nature Climate Change*.
- Sinclair, S.J., White, M.D., Newell, G.R. *et al.* (2010). How useful are species distribution models for managing biodiversity under future climates. *Ecology and Society*, vol. 15, no. 8.
- Stanger, K. (2006). Algorithms for generating fractal landscapes. *Ecology Letters*, vol. 1, no. 3, pp. 1–23.
- Suarez, A.V., Holway, D.A. and Case, T.J. (2001). Patterns of spread in biological invasions dominated by long-distance jump dispersal: insights from Argentine ants. *Proceedings of the National Academy of Sciences*, vol. 98, no. 3, pp. 1095–1100.
- Turchin, P. and Hall, T.D. (2015). Spatial synchrony among and within world-systems: insights from theoretical ecology. *Journal of World-Systems Research*, vol. 9, no. 1, pp. 37–64.
- Turner, M.G. (1989). Landscape ecology: the effect of pattern on process. *Annual Review of Ecology and Systematics*, pp. 171–197.
- Walsh, C., Mac Nally, R. and Walsh, M.C. (2003). The hier. part package. *Hierarchical Partitioning. R Project for Statistical Computing*. URL: <http://cran.r-project.org>.

- Warnes, G.R., Bolker, B., Bonebakker, L., Gentleman, R., Huber, W., Liaw, A., Lumley, T., Maechler, M., Magnusson, A., Moeller, S. *et al.* (2013). *gplots*: Various r programming tools for plotting data. r package version 2.12. 1.
- Warnes, G.R., Bolker, B., Gorjanc, G., Grothendieck, G., Korosec, A., Lumley, T., MacQueen, D., Magnusson, A., Rogers, J. *et al.* (2014). *gdata*: Various r programming tools for data manipulation.
- Wiens, J.A. (1989). Spatial scaling in ecology. *Functional Ecology*, vol. 3, no. 4, pp. 385–397.
- Wisz, M.S., Pottier, J., Kissling, W.D., Pellissier, L., Lenoir, J., Damgaard, C.F., Dormann, C.F., Forchhammer, M.C., Grytnes, J.-A., Guisan, A. *et al.* (2013). The role of biotic interactions in shaping distributions and realised assemblages of species: implications for species distribution modelling. *Biological Reviews*, vol. 88, no. 1, pp. 15–30.
- Wu, J., Jones, B., Li, H. and Loucks, O.L. (2006). *Scaling and uncertainty analysis in ecology*, chap. methods and applications. Wiley Online Library, Oxford.
- Wu, J. and Li, H. (2006). Concepts of scale and scaling. In: *Scaling and uncertainty analysis in ecology*, pp. 3–15. Springer.